

VIBRATIONAL CONTRIBUTIONS  
TO THE SECOND HYPERPOLARIZABILITY OF  $CF_4$


BY

ZHENGFANG LU

A THESIS

SUBMITTED TO THE FACULTY OF  
GRADUATE STUDIES IN PARTIAL FULFILMENT  
OF THE REQUIREMENTS FOR THE DEGREE  
OF MASTER OF SCIENCE IN

PHYSICS

MARCH 1987 

Permission has been granted to the National Library of Canada to microfilm this thesis and to lend or sell copies of the film.

The author (copyright owner) has reserved other publication rights, and neither the thesis nor extensive extracts from it may be printed or otherwise reproduced without his/her written permission.

L'autorisation a été accordée à la Bibliothèque nationale du Canada de microfilmer cette thèse et de prêter ou de vendre des exemplaires du film.

L'auteur (titulaire du droit d'auteur) se réserve les autres droits de publication; ni la thèse ni de longs extraits de celle-ci ne doivent être imprimés ou autrement reproduits sans son autorisation écrite.

ISBN 0-315-37464-0

THE UNIVERSITY OF MANITOBA LIBRARIES

VIBRATIONAL CONTRIBUTIONS TO THE SECOND  
HYPERPOLARIZABILITY OF  $\text{CF}_4$

BY

ZHENGFANG LU

A thesis submitted to the Faculty of Graduate Studies of  
the University of Manitoba in partial fulfillment of the requirements  
of the degree of

MASTER OF SCIENCE

© 1987

Permission has been granted to the LIBRARY OF THE UNIVERSITY OF MANITOBA to lend or sell copies of this thesis, to the NATIONAL LIBRARY OF CANADA to microfilm this thesis and to lend or sell copies of the film, and UNIVERSITY MICROFILMS to publish an abstract of this thesis.

The author reserves other publication rights, and neither the thesis nor extensive extracts from it may be printed or otherwise reproduced without the author's written permission.

## ACKNOWLEDGEMENT

I am grateful to my supervisor, Dr. D.P. Shelton for his patience, encouragement and very friendly guidance throughout the whole period of this study. The friendship has made the cold day in Winnipeg become enjoyable.

## ABSTRACT

The frequency dependence of the second hyperpolarizability ( $\gamma$ ) of  $\text{CF}_4$  has been measured in the visible ( $488 \text{ nm} < \lambda < 660 \text{ nm}$ ) by means of gas-phase electric-field-induced second harmonic generation (ESHG). The results of these experiments are compared with the results of other nonlinear optics experiments which have measured  $\gamma$  by third harmonic generation (THG), ESHG and the dc Kerr effect. In order to obtain information about the vibrational contributions to the second hyperpolarizability from this comparison, expressions for the vibrational contributions to  $\gamma\text{CF}_4$  have been derived and numerically evaluated for each of these optical processes. It is concluded that vibrational contributions to  $\gamma\text{CF}_4$  are negligible for THG, but significant for both the dc Kerr effect and ESHG.

## CONTENTS

Acknowledgement .....	i
Abstract .....	ii
Chapter 1 Introduction: History and Present Interest ...	1
Chapter 2 Theory .....	4
2.1 Quantum Mechanical Expression For The Second Hyperpolarizability .....	4
2.2 Expression For $\gamma_{\text{THG}}^{\text{V}}$ For $\text{CF}_4$ .....	8
2.3 Expression For $\gamma_{\text{ESHG}}^{\text{V}}$ For $\text{CF}_4$ .....	12
2.4 Expression For $\gamma_{\text{Kerr}}^{\text{V}}$ For $\text{CF}_4$ .....	17
Chapter 3 Experiment .....	26
3.1 Experimental System For dc ESHG .....	26
3.2 Sample Preparation And Effect Of Impurities .....	29
3.3 Signal Curve And Data Analysis .....	31
Chapter 4 Experiment Results .....	38
4.1 Local Field Correction Factor .....	38
4.2 Dispersion Of The Second Hyperpolarizability Of $\text{CF}_4$ From ESHG Experiment .....	42

Chapter 5 Discussion: $\gamma_{\text{THG}}^{\text{V}}$ , $\gamma_{\text{ESHG}}^{\text{V}}$ And $\gamma_{\text{Kerr}}^{\text{V}}$ For $\text{CF}_4$ .....	48
5.1 $\gamma_{\text{THG}}^{\text{V}}$ And $\gamma_{\text{ESHG}}^{\text{V}}$ For $\text{CF}_4$ .....	48
5.1.1 Previous Results Of $\gamma_{\text{CF}_4}$ In THG, ESHG And The Kerr Effect .....	48
5.1.2 $\gamma_{\text{THG}}^{\text{V}}$ And $\gamma_{\text{ESHG}}^{\text{V}}$ For $\text{CF}_4$ .....	51
5.1.3 Hyper-Raman $\beta$ .....	54
5.2 $\gamma_{\text{Kerr}}^{\text{V}}$ For $\text{CF}_4$ .....	56
5.2.1 The Nature Of The Vibrations For $\text{CF}_4$ .....	56
5.2.2 $\gamma_{\text{Kerr}}^{\text{V}}$ -- Significant But Not Large .....	58
Chapter 6 Conclusion .....	70
References .....	72
Appendix Programs For The Calculations In The Thesis ...	76
Index Of Figures	
Figure 2.1 Diagrams For The Five Essential Types Of Terms Which Contribute To $\gamma^{\text{V}}$ .....	24
Figure 3.1 Experimental System .....	34
Figure 3.2 Signal Curve And Least Squares Fitting Polynomial .....	36

Figure 4.1	The Measured Values of $\gamma_{CF_4}$ By ESHG	44
Figure 5.1	$\gamma_{CF_4}$ Measured By Several Nonlinear Optical Processes	61
Figure 5.2	The Normal Vibrations Of $CF_4$	63

Index Of Tables

Table 4.1	Local Field Correction Factor	46
Table 4.2	Experimental Results For $\gamma_{CF_4}$	47
Table 5.1	$\gamma_{CF_4}$ Measured By Several Nonlinear Optical Processes	50
Table 5.2	Matrix Elements	65



## CHAPTER 1

## INTRODUCTION: HISTORY AND PRESENT INTEREST

The world we are living in is a "nonlinear" colorful world. Studies of nonlinear phenomena have a long history. Even in optics, the Faraday effect was discovered in 1845 and the Kerr effect in 1875. "Nonlinear optics" is usually used to refer to those phenomena involving light waves, which must be described in terms containing other than the first power of the electric and magnetic field strengths. In physics, many important phenomena depend on the electric dipole moments induced in atoms or molecules by externally applied electric fields. On the other hand, many nonlinear optical processes can provide much information related to the polarizability and hyperpolarizability. However, since nonlinear optical phenomena are really observable only if the electric field is large enough for the nonlinearity of the polarization to appear, nonlinear optics became a subject of great common interest only after the laser was invented.<sup>1</sup> The remarkable first observation of a nonlinear optical effect was made by Franken, Hill, Peters and Weinreich in 1961 when they observed optical second-harmonic

generation (SHG) using a ruby laser. Since then many important nonlinear optical processes including third-harmonic generation (THG), the dc Kerr effect and four-wave mixing (FWM) have been widely observed in solids, liquids and gases.<sup>1,2</sup> At the same time a number of semi-classical theoretical treatments of high order polarizabilities including those by Bloembergen et al. in 1962 and Ward in 1965 appeared.<sup>1,3,4</sup>

Here, what we are concerned about is the vibrational contribution to the second hyperpolarizability of a certain molecule. The third-order nonlinear susceptibility  $\chi^{(3)}$ , which mediates a wide range of nonlinear-optical processes, is the macroscopic expression of the microscopic second hyperpolarizability tensor  $\gamma^{1-4}$ . Perturbation theory gives a single expression for  $\gamma$ , and the hyperpolarizabilities corresponding to each of the various nonlinear optical processes are just special cases of this general expression.<sup>5-7</sup> The underlying unity of the fundamental theoretical description is obscured in practice because  $\gamma$  for each nonlinear optical process has a characteristically different balance of contributions from the electronic, vibrational and rotational degrees of freedom of each molecule.<sup>8-10</sup> Recently there has been much theoretical interest and

activity directed towards gaining an understanding of the various contributions to  $\gamma$  for various small molecules by means of ab initio calculations.<sup>11-15</sup> On the other hand, since the particular  $\gamma$  tensors mediating the various processes are merely instances of a general  $\gamma$  tensor differing only in their frequency arguments, it should be possible to disentangle the contributions of the various molecular mechanisms by experimentally studying the frequency dependence of  $\gamma$ . In this thesis we will present experimental measurements of the frequency dependence of  $\gamma$  for  $\text{CF}_4$  made by means of electric-field-induced second harmonic generation (ESHG) and a comparison of these results with the results of previous measurements from several other nonlinear-optics experiments on the same molecule. In order to get information about the vibrational contributions to the second hyperpolarizability from this comparison, we have also derived and numerically evaluated the expressions of vibrational contributions to  $\gamma_{\text{CF}_4}$  for the nonlinear-optical processes of THG, ESHG and the dc Kerr effect.

CHAPTER 2  
VIBRATIONAL CONTRIBUTION  
TO THE SECOND HYPERPOLARIZABILITY

The theory applied in this work includes two parts: one is the theory of hyperpolarizability in which we are interested, and the other is the theory by which the molecular hyperpolarizability is extracted from our experimental observations of dc electric-field-induced second-harmonic generation (ESHG). Details of the latter can be found in Refs.(16-20). In this chapter we will derive the expressions for vibrational contributions to the second hyperpolarizability for different nonlinear optical process.

2.1 ... Quantum Mechanical Expression For The Second Hyperpolarizability

Hyperpolarizability has been well studied using quantum mechanical theory during the 1970's. Equivalent expressions for the hyperpolarizability have been derived using perturbation theory with the help of the method of

averages, the density matrix or Feynman diagrams.<sup>1,5</sup> The expression of  $\gamma$  used as a starting point here is from perturbation theory and the average method due to Orr and Ward in 1971.<sup>5</sup> This expression is applicable when damping may be ignored and is suitable for use even in the static limit:

$$\begin{aligned} \gamma_{\alpha\beta\gamma\delta}(-\omega_{\sigma}; \omega_1, \omega_2, \omega_3) &= \hbar^{-3} \sum_P \\ &\times \left\{ \sum'_m \sum'_n \sum'_p \frac{\langle g|\mu_{\alpha}|m\rangle \langle m|\mu_{\delta}|n\rangle \langle n|\mu_{\gamma}|p\rangle \langle p|\mu_{\beta}|g\rangle}{(\Omega_{mg} - \omega_{\sigma})(\Omega_{ng} - \omega_1 - \omega_2)(\Omega_{pg} - \omega_1)} \right. \\ &\quad \left. - \sum'_m \sum'_n \frac{\langle g|\mu_{\alpha}|m\rangle \langle m|\mu_{\delta}|g\rangle \langle g|\mu_{\gamma}|n\rangle \langle n|\mu_{\beta}|g\rangle}{(\Omega_{mg} - \omega_{\sigma})(\Omega_{ng} - \omega_1)(\Omega_{ng} + \omega_2)} \right\} \end{aligned} \quad (2.1.1)$$

where

$$\omega_{\sigma} = \omega_1 + \omega_2 + \omega_3, \quad (2.1.2)$$

and  $\sum_P$  denotes the sum over terms obtained by permuting the frequencies  $-\omega_{\sigma}$ ,  $\omega_1$ ,  $\omega_2$  and  $\omega_3$ , together with their associated spatial subscripts  $\alpha$ ,  $\beta$ ,  $\gamma$  and  $\delta$ . The primed sums over intermediate states exclude the ground state  $|g\rangle$ . This expression is valid for nondipolar molecules such as  $\text{CF}_4$ . For arbitrary  $\omega_1$ ,  $\omega_2$  and  $\omega_3$ , Eq.(2.1.1) gives 48 permuted terms as follows:





The vibrational contribution to the total  $\gamma$  is the sum of all those terms for which at least one of the intermediate states is a vibrationally excited state in the ground electronic manifold of states.<sup>9,21</sup>

## 2.2 ... Expression For $\gamma_{\text{THG}}^{\text{V}}$ For $\text{CF}_4$

In the case of third-harmonic generation (THG) the vibrational hyperpolarizability  $\gamma^{\text{V}}$  is obtained by substituting

$$(-\omega_0; \omega_1, \omega_2, \omega_3) = (-3\omega; \omega, \omega, \omega) \quad (2.2.1)$$

to get the 48 permuted terms:

$$\begin{aligned} & \sum_{m,n,p} \frac{\langle g | \mu_\alpha | m \rangle \langle m | \mu_\delta | n \rangle \langle n | \mu_\gamma | p \rangle \langle p | \mu_\beta | g \rangle}{(\Omega m g - 3\omega)(\Omega n g - 2\omega)(\Omega p g - \omega)} - \sum_{m,n} \frac{\langle g | \mu_\alpha | m \rangle \langle m | \mu_\delta | g \rangle \langle g | \mu_\gamma | n \rangle \langle n | \mu_\beta | g \rangle}{(\Omega m g - 3\omega)(\Omega n g - \omega)(\Omega n g + \omega)} \\ & \sum_{m,n,p} \frac{\langle g | \mu_\alpha | m \rangle \langle m | \mu_\gamma | n \rangle \langle n | \mu_\delta | p \rangle \langle p | \mu_\beta | g \rangle}{(\Omega m g - 3\omega)(\Omega n g - 2\omega)(\Omega p g - \omega)} - \sum_{m,n} \frac{\langle g | \mu_\alpha | m \rangle \langle m | \mu_\gamma | g \rangle \langle g | \mu_\delta | n \rangle \langle n | \mu_\beta | g \rangle}{(\Omega m g - 3\omega)(\Omega n g - \omega)(\Omega n g + \omega)} \\ & \sum_{m,n,p} \frac{\langle g | \mu_\alpha | m \rangle \langle m | \mu_\delta | n \rangle \langle n | \mu_\beta | p \rangle \langle p | \mu_\gamma | g \rangle}{(\Omega m g - 3\omega)(\Omega n g - 2\omega)(\Omega p g - \omega)} - \sum_{m,n} \frac{\langle g | \mu_\alpha | m \rangle \langle m | \mu_\delta | g \rangle \langle g | \mu_\beta | n \rangle \langle n | \mu_\gamma | g \rangle}{(\Omega m g - 3\omega)(\Omega n g - \omega)(\Omega n g + \omega)} \\ & \sum_{m,n,p} \frac{\langle g | \mu_\alpha | m \rangle \langle m | \mu_\beta | n \rangle \langle n | \mu_\delta | p \rangle \langle p | \mu_\gamma | g \rangle}{(\Omega m g - 3\omega)(\Omega n g - 2\omega)(\Omega p g - \omega)} - \sum_{m,n} \frac{\langle g | \mu_\alpha | m \rangle \langle m | \mu_\beta | g \rangle \langle g | \mu_\delta | n \rangle \langle n | \mu_\gamma | g \rangle}{(\Omega m g - 3\omega)(\Omega n g - \omega)(\Omega n g + \omega)} \\ & \sum_{m,n,p} \frac{\langle g | \mu_\alpha | m \rangle \langle m | \mu_\beta | n \rangle \langle n | \mu_\gamma | p \rangle \langle p | \mu_\delta | g \rangle}{(\Omega m g - 3\omega)(\Omega n g - 2\omega)(\Omega p g - \omega)} - \sum_{m,n} \frac{\langle g | \mu_\alpha | m \rangle \langle m | \mu_\beta | g \rangle \langle g | \mu_\gamma | n \rangle \langle n | \mu_\delta | g \rangle}{(\Omega m g - 3\omega)(\Omega n g - \omega)(\Omega n g + \omega)} \\ & \sum_{m,n,p} \frac{\langle g | \mu_\alpha | m \rangle \langle m | \mu_\gamma | n \rangle \langle n | \mu_\beta | p \rangle \langle p | \mu_\delta | g \rangle}{(\Omega m g - 3\omega)(\Omega n g - 2\omega)(\Omega p g - \omega)} - \sum_{m,n} \frac{\langle g | \mu_\alpha | m \rangle \langle m | \mu_\gamma | g \rangle \langle g | \mu_\beta | n \rangle \langle n | \mu_\delta | g \rangle}{(\Omega m g - 3\omega)(\Omega n g - \omega)(\Omega n g + \omega)} \\ & \sum_{m,n,p} \frac{\langle g | \mu_\beta | m \rangle \langle m | \mu_\delta | n \rangle \langle n | \mu_\gamma | p \rangle \langle p | \mu_\alpha | g \rangle}{(\Omega m g + \omega)(\Omega n g + 2\omega)(\Omega p g + 3\omega)} - \sum_{m,n} \frac{\langle g | \mu_\beta | m \rangle \langle m | \mu_\delta | g \rangle \langle g | \mu_\gamma | n \rangle \langle n | \mu_\alpha | g \rangle}{(\Omega m g + \omega)(\Omega n g + 3\omega)(\Omega n g + \omega)} \end{aligned}$$





Each of these terms may be classified according to whether one, two or three of the intermediate states  $m, n, p$  are vibrationally excited states of the ground electronic manifold. Thus, seven distinct groups of terms arise from each of the permuted terms of Eq.(2.1.1) involving the triple sum over states, while only three groups of terms arise from each of the permuted terms of Eq.(2.1.1) involving the double sum over states. The THG signal measured in the laboratory is related to the XXXX component of the isotropically averaged molecular hyperpolarizability tensor. If the dominant contributions to the hyperpolarizabilities are from transitions whose frequencies are remote from all relevant field and polarization frequencies, then Kleinman symmetry applies and the hyperpolarizabilities are approximately invariant to interchange of polarization and field coordinate subscripts.<sup>4</sup> In the special case of third-harmonic generation, it may be noted that Kleinman symmetry holds exactly due to the intrinsic permutation symmetry ( $\omega_1 = \omega_2 = \omega_3 = \omega$ )<sup>18</sup>. Furthermore, since the x, y, z directions are equivalent for a  $T_d$  symmetry group molecule such as  $CF_4$ , one may write

$$\gamma_{THG} = \langle \gamma \rangle_{XXXX} = \gamma_{xxxx} - 2/5 \Delta\gamma, \quad (2.2.3)$$

where  $\langle \rangle$  denotes the isotropic average,

$$\Delta\gamma = ( \gamma_{xxxx} - 3\gamma_{xxyy} ) \quad , \quad (2.2.4)$$

and the upper case (lower case) spatial indices refer to the laboratory (molecular) frame. For an atom  $\Delta\gamma = 0$ . At the present level of approximation it should be adequate to assume  $\Delta\gamma = 0$  for  $\text{CF}_4$  as well, from which it follows that  $\gamma_{\text{THG}}^{\text{Y}} = \gamma_{\text{xxxx}}^{\text{V}}$ . By considering only the tensor component  $\gamma_{\text{xxxx}}$ , the number of distinct terms is reduced from 240 to just 40.

In order to proceed further in evaluating  $\gamma_{\text{THG}}^{\text{Y}}$ , one notes that the following approximate relations hold for the transition frequencies and dipole matrix elements of the principal electronic and vibrational transitions for  $\text{CF}_4$ :

$$\Omega_e \sim 10 \omega \sim 100 \Omega_v \quad (2.2.5a)$$

$$|\mu_e| \approx 10 |\mu_v| \quad (2.2.5b)$$

$$|\mu_e|^2 / \Omega_e \approx |\mu_v|^2 / \Omega_v \quad (2.2.5c)$$

where  $\Omega_e$ ,  $\omega$ ,  $\Omega_v$ , are electronic, optical and vibrational transition frequencies and  $\mu_e$  and  $\mu_v$  are typical electronic and vibrational transition matrix elements. Eq.(2.2.5c) follows from Eq.(2.2.5a) and (2.2.5b) and it essentially states that the electronic and vibrational contributions to the static polarizability are about equal. Characterizing all the electronic and vibrational transitions by  $\mu_e$ ,  $\Omega_e$  and  $\mu_v$ ,  $\Omega_v$  is a crude approximation, but it allows one to easily

obtain a simple result for  $\gamma_{\text{THG}}^{\text{V}}$ . From Eq.(2.2.5a), the denominators of the terms in the expression for  $\gamma_{\text{THG}}^{\text{V}}$  may be written so as to involve only  $\Omega_{\text{V}}$ :

$$\begin{aligned}\Omega_{\text{V}} - 3\omega &\approx -3\Omega_{\text{V}} \times 10, \\ \Omega_{\text{e}} - 3\omega &\approx \Omega_{\text{V}} \times 100, \text{ etc.}\end{aligned}\quad (2.2.6)$$

Similarly, employing Eq.(2.2.3) allows one to write all the numerators so that they involve only  $\mu_{\text{V}}$  (ie.  $\langle g|\mu|m\rangle \approx 10\mu_{\text{V}}$  if gm is an electronic transition). Then every term of  $\gamma_{\text{THG}}^{\text{V}}$  is simply proportional to  $\mu_{\text{V}}^4/\Omega_{\text{V}}^3$ . The terms arising from the triple sum over states in Eq.(2.1.1) all sum to zero, while the term inside the double sum in Eq.(2.1.1) gives just  $(-64/1000) \mu_{\text{V}}^4/\Omega_{\text{V}}^3$ . Thus, one obtains the following expression for  $\gamma_{\text{THG}}^{\text{V}}$ :

$$\gamma_{\text{THG}}^{\text{V}} = (64/1000) (\sum_{\text{m}} |\mu_{\text{mg}}^{\text{X}}|^2)^2 / (\pi \Omega_{\text{V}})^3. \quad (2.2.7)$$

As mentioned before this derivation uses some relatively crude approximations, but it is still significant because at least it allows one to estimate the order of magnitude of  $\gamma_{\text{THG}}^{\text{V}}$ .

### 2.3 ... Expression For $\gamma_{\text{ESHG}}^{\text{V}}$ For $\text{CF}_4$

In the case of ESHG, the situation is rather different from that of THG. Substituting

$$(\omega_0; \omega_1, \omega_2, \omega_3) = (-2\omega; \omega, \omega, 0), \quad (2.3.1)$$

one may again write out the 48 permuted terms and one finds that more than half of the terms have the factors  $(\Omega_V - \omega^-)$  in the denominator with  $\omega^- = 0$  (indicated by \* on the top left of the terms):

$$\begin{aligned} & \sum_{m,n,p} \frac{\langle g | \mu_\alpha | m \rangle \langle m | \mu_\delta | n \rangle \langle n | \mu_\gamma | p \rangle \langle p | \mu_\beta | g \rangle}{(\Omega m g - 2\omega)(\Omega n g - 2\omega)(\Omega p g - \omega)} - \sum_{m,n} \frac{\langle g | \mu_\alpha | m \rangle \langle m | \mu_\delta | g \rangle \langle g | \mu_\gamma | n \rangle \langle n | \mu_\beta | g \rangle}{(\Omega m g - 2\omega)(\Omega n g - \omega)(\Omega n g + \omega)} \\ & \sum_{m,n,p} \frac{\langle g | \mu_\alpha | m \rangle \langle m | \mu_\gamma | n \rangle \langle n | \mu_\delta | p \rangle \langle p | \mu_\beta | g \rangle}{(\Omega m g - 2\omega)(\Omega n g - \omega)(\Omega p g - \omega)} - \sum_{m,n}^* \frac{\langle g | \mu_\alpha | m \rangle \langle m | \mu_\gamma | g \rangle \langle g | \mu_\delta | n \rangle \langle n | \mu_\beta | g \rangle}{\Omega m g - 2\omega)(\Omega n g - \omega)(\Omega n g)} \\ & \sum_{m,n,p} \frac{\langle g | \mu_\alpha | m \rangle \langle m | \mu_\delta | n \rangle \langle n | \mu_\beta | p \rangle \langle p | \mu_\gamma | g \rangle}{(\Omega m g - 2\omega)(\Omega n g - 2\omega)(\Omega p g - \omega)} - \sum_{m,n} \frac{\langle g | \mu_\alpha | m \rangle \langle m | \mu_\delta | g \rangle \langle g | \mu_\beta | n \rangle \langle n | \mu_\gamma | g \rangle}{(\Omega m g - 2\omega)(\Omega n g - \omega)(\Omega n g + \omega)} \\ & \sum_{m,n,p} \frac{\langle g | \mu_\alpha | m \rangle \langle m | \mu_\beta | n \rangle \langle n | \mu_\delta | p \rangle \langle p | \mu_\gamma | g \rangle}{(\Omega m g - 2\omega)(\Omega n g - \omega)(\Omega p g - \omega)} - \sum_{m,n}^* \frac{\langle g | \mu_\alpha | m \rangle \langle m | \mu_\beta | g \rangle \langle g | \mu_\delta | n \rangle \langle n | \mu_\gamma | g \rangle}{(\Omega m g - 2\omega)(\Omega n g - \omega)(\Omega n g)} \\ & \sum_{m,n,p}^* \frac{\langle g | \mu_\alpha | m \rangle \langle m | \mu_\beta | n \rangle \langle n | \mu_\gamma | p \rangle \langle p | \mu_\delta | g \rangle}{(\Omega m g - 2\omega)(\Omega n g - \omega)(\Omega p g)} - \sum_{m,n}^* \frac{\langle g | \mu_\alpha | m \rangle \langle m | \mu_\beta | g \rangle \langle g | \mu_\gamma | n \rangle \langle n | \mu_\delta | g \rangle}{(\Omega m g - 2\omega)(\Omega n g)(\Omega n g + \omega)} \\ & \sum_{m,n,p}^* \frac{\langle g | \mu_\alpha | m \rangle \langle m | \mu_\gamma | n \rangle \langle n | \mu_\beta | p \rangle \langle p | \mu_\delta | g \rangle}{(\Omega m g - 2\omega)(\Omega n g - \omega)(\Omega p g)} - \sum_{m,n}^* \frac{\langle g | \mu_\alpha | m \rangle \langle m | \mu_\gamma | g \rangle \langle g | \mu_\beta | n \rangle \langle n | \mu_\delta | g \rangle}{(\Omega m g - 2\omega)(\Omega n g)(\Omega n g + \omega)} \\ \\ & \sum_{m,n,p} \frac{\langle g | \mu_\beta | m \rangle \langle m | \mu_\delta | n \rangle \langle n | \mu_\gamma | p \rangle \langle p | \mu_\alpha | g \rangle}{(\Omega m g + \omega)(\Omega n g + \omega)(\Omega p g + 2\omega)} - \sum_{m,n} \frac{\langle g | \mu_\beta | m \rangle \langle m | \mu_\delta | g \rangle \langle g | \mu_\gamma | n \rangle \langle n | \mu_\alpha | g \rangle}{(\Omega m g + \omega)(\Omega n g + 2\omega)(\Omega n g + \omega)} \\ & \sum_{m,n,p} \frac{\langle g | \mu_\beta | m \rangle \langle m | \mu_\gamma | n \rangle \langle n | \mu_\delta | p \rangle \langle p | \mu_\alpha | g \rangle}{(\Omega m g + \omega)(\Omega n g + 2\omega)(\Omega p g + 2\omega)} - \sum_{m,n}^* \frac{\langle g | \mu_\beta | m \rangle \langle m | \mu_\gamma | g \rangle \langle g | \mu_\delta | n \rangle \langle n | \mu_\alpha | g \rangle}{(\Omega m g + \omega)(\Omega n g + 2\omega)(\Omega n g)} \\ & \sum_{m,n,p} \frac{\langle g | \mu_\beta | m \rangle \langle m | \mu_\delta | n \rangle \langle n | \mu_\alpha | p \rangle \langle p | \mu_\gamma | g \rangle}{(\Omega m g + \omega)(\Omega n g + \omega)(\Omega p g - \omega)} - \sum_{m,n} \frac{\langle g | \mu_\beta | m \rangle \langle m | \mu_\delta | g \rangle \langle g | \mu_\alpha | n \rangle \langle n | \mu_\gamma | g \rangle}{(\Omega m g + \omega)(\Omega n g - \omega)(\Omega n g - 2\omega)} \\ & \sum_{m,n,p} \frac{\langle g | \mu_\beta | m \rangle \langle m | \mu_\alpha | n \rangle \langle n | \mu_\delta | p \rangle \langle p | \mu_\gamma | g \rangle}{(\Omega m g + \omega)(\Omega n g - \omega)(\Omega p g - \omega)} - \sum_{m,n}^* \frac{\langle g | \mu_\beta | m \rangle \langle m | \mu_\alpha | g \rangle \langle g | \mu_\delta | n \rangle \langle n | \mu_\gamma | g \rangle}{(\Omega m g + \omega)(\Omega n g - \omega)(\Omega n g)} \\ & \sum_{m,n,p}^* \frac{\langle g | \mu_\beta | m \rangle \langle m | \mu_\alpha | n \rangle \langle n | \mu_\gamma | p \rangle \langle p | \mu_\delta | g \rangle}{(\Omega m g + \omega)(\Omega n g - \omega)(\Omega p g)} - \sum_{m,n}^* \frac{\langle g | \mu_\beta | m \rangle \langle m | \mu_\alpha | g \rangle \langle g | \mu_\gamma | n \rangle \langle n | \mu_\delta | g \rangle}{(\Omega m g + \omega)(\Omega n g)(\Omega n g + \omega)} \end{aligned}$$



Since for typical vibrational and optical frequencies,  $\Omega_v \ll \omega$ , terms with a factor of the form  $(\Omega_v - 0)$  in the denominator will be strongly enhanced over all the other terms. Retaining only enhanced terms one obtains the following expressions for the relevant tensor components of  $\gamma_{\text{ESHG}}^V$ :

$$\begin{aligned}
 & \gamma_{\alpha\beta\beta\alpha}^V(-2\omega; \omega, \omega, 0) \\
 &= \hbar^{-1} \sum_m' \frac{2\mu_{gm}^\alpha (\beta_{\alpha\beta\beta})_{mg}}{\Omega_{mg}} \\
 &+ \hbar^{-3} \sum_m' \sum_n' \left\{ \frac{\mu_{gm}^\alpha \mu_{mg}^\alpha \mu_{gn}^\beta \mu_{ng}^\beta + 2\mu_{gm}^\alpha \mu_{mg}^\beta \mu_{gn}^\beta \mu_{ng}^\alpha}{\omega^3} \right. \\
 &\quad \left. + \frac{2\mu_{gm}^\alpha \mu_{mg}^\alpha \mu_{gn}^\beta \mu_{ng}^\beta - 2\mu_{gm}^\alpha \mu_{mg}^\beta \mu_{gn}^\beta \mu_{ng}^\alpha}{\Omega_{mg} \omega^2} \right\}
 \end{aligned}
 \tag{2.3.3}$$

and

$$\begin{aligned}
 & \gamma_{\alpha\beta\alpha\beta}^V(-2\omega; \omega, \omega, 0) = \gamma_{\alpha\alpha\beta\beta}^V(-2\omega; \omega, \omega, 0) \\
 &= \hbar^{-1} \sum_m' \frac{\mu_{gm}^\beta (\beta_{\alpha\alpha\beta})_{mg} + \mu_{gm}^\beta (\beta_{\beta\alpha\alpha})_{mg}}{\Omega_{mg}} \\
 &+ \hbar^{-3} \sum_m' \sum_n' \left\{ \frac{2\mu_{gm}^\beta \mu_{mg}^\alpha \mu_{gn}^\alpha \mu_{ng}^\beta + \mu_{gm}^\beta \mu_{mg}^\beta \mu_{gn}^\alpha \mu_{ng}^\alpha}{\omega^3} \right. \\
 &\quad \left. + \frac{\mu_{gm}^\beta \mu_{mg}^\alpha \mu_{gn}^\alpha \mu_{ng}^\beta - \mu_{gm}^\beta \mu_{mg}^\beta \mu_{gn}^\alpha \mu_{ng}^\alpha}{\Omega_{mg} \omega^2} \right\}
 \end{aligned}
 \tag{2.3.4}$$

where  $|m\rangle$ ,  $|n\rangle$  are vibrational excited states of the ground

electronic manifold, and  $(\beta_{\alpha\beta\gamma})_{gp}$  are components of the hyper-Raman transition hyperpolarizability tensor defined by<sup>22</sup>

$$(\beta_{\alpha\beta\gamma})_{gp} = 2\hbar^{-2} \sum_m' \sum_n' \left\{ \frac{\langle g|\mu_\beta|m\rangle\langle m|\mu_\alpha|n\rangle\langle n|\mu_\gamma|p\rangle}{(\Omega_{mg} + \omega)(\Omega_{ng} - \omega)} + \frac{\langle g|\mu_\beta|m\rangle\langle m|\mu_\gamma|n\rangle\langle n|\mu_\alpha|p\rangle}{(\Omega_{mg} + \omega)(\Omega_{ng} + 2\omega)} + \frac{\langle g|\mu_\gamma|m\rangle\langle m|\mu_\beta|n\rangle\langle n|\mu_\alpha|p\rangle}{(\Omega_{mg} - 2\omega)(\Omega_{ng} - \omega)} \right\} .$$

(2.3.5)

The experimentally measured quantity in our ESHG experiment is  $\langle\gamma\rangle_{XXXX}$ . The isotropically averaged  $\gamma$  tensors for ESHG and the dc Kerr effect have only two independent components:  $\langle\gamma\rangle_{XXXX}$  and  $\langle\gamma\rangle_{XYYX}$ . For both ESHG and the dc Kerr effect the relation

$$\langle\gamma\rangle_{XXYY} = \langle\gamma\rangle_{XYYX} \quad (2.3.6a)$$

holds, as well as the more general relation

$$\langle\gamma\rangle_{XXXX} = \langle\gamma\rangle_{XXYY} + \langle\gamma\rangle_{XYYX} + \langle\gamma\rangle_{XYYX} . \quad (2.3.6b)$$

Making use of the equivalence of the x, y, z directions for a tetrahedral molecule, one may write the two independent components of  $\langle\gamma\rangle$  in terms of the three independent components of  $\gamma$  as follows:

$$\langle\gamma\rangle_{XXXX} = 1/5 ( 3\gamma_{xxxx} + 4\gamma_{xxyy} + 2\gamma_{xyyx} ) \quad (2.3.6c)$$

$$\langle\gamma\rangle_{XYYX} = 1/5 ( \gamma_{xxxx} - 2\gamma_{xxyy} + 4\gamma_{xyyx} ) \quad (2.3.6d)$$



where the lower case indices denote components in the molecule fixed frame. Substituting Eqs.(2.3.3, 2.3.4) into Eqs.(2.3.6c, d), and considering that for the spherical top molecule  $CF_4$  the following relations are satisfied:<sup>23, 25</sup>

$$\beta_{xxx} = \beta_{yyy} = \beta_{zzz} \quad (2.3.7a)$$

$$\beta_{xyy} + \beta_{zzx} = \beta_{yzz} + \beta_{xxy} = \beta_{zxx} + \beta_{yyz} \quad (2.3.7b)$$

$$\beta_{xyy} = \beta_{yyx}, \beta_{xzz} = \beta_{zzx}, \beta_{yzz} = \beta_{zzy} \quad (2.3.7c)$$

one obtains the following expression of  $\gamma_{ESHG}^V$  for  $CF_4$ :

$$\begin{aligned} \gamma_{ESHG}^V = & \frac{12}{5} \hbar^{-1} \sum_m' \frac{\mu_{gm}^x (\beta_{xxx} + \beta_{xyy} + \beta_{zzx}) \omega_{mg}}{\omega_{mg}} \\ & + \frac{27}{5} \hbar^{-3} \sum_m' \sum_n' \frac{|\mu_{gm}^x|^2 |\mu_{gn}^x|^2}{\omega^3} \end{aligned} \quad (2.3.8)$$

At optical frequencies, the second term of Eq.(2.3.8) should be very small and the first term is expected to be dominant.

#### 2.4 ... Expression For $\gamma_{Kerr}^V$ For $CF_4$

The second hyperpolarizability related to the dc Kerr effect is defined by

$$\gamma_{\text{Kerr}} = (-\omega; 0, 0, \omega) \quad (2.4.1)$$

Substituting

$$(-\omega; \omega_1, \omega_2, \omega_3) = (-\omega; 0, 0, \omega)$$

in Eq.(2.1.1), one can also write out the 48 frequency permuted terms for  $\gamma_{\text{Kerr}}^V$ . One finds that in this case there appear terms with two of the factors  $(\Omega_V - \omega')$  in the denominator having  $\omega' = 0$  (indicated by \*\* on the top left of the terms):

$$\begin{aligned} & \sum_{m,n,p}^{**} \frac{\langle g | \mu_\alpha | m \rangle \langle m | \mu_\delta | n \rangle \langle n | \mu_\gamma | p \rangle \langle p | \mu_\beta | g \rangle}{(\Omega_{mg} - \omega)(\Omega_{ng})(\Omega_{pg})} - \sum_{m,n}^{**} \frac{\langle g | \mu_\alpha | m \rangle \langle m | \mu_\delta | g \rangle \langle g | \mu_\gamma | n \rangle \langle n | \mu_\beta | g \rangle}{\Omega_{mg} - \omega)(\Omega_{ng})(\Omega_{ng})} \\ & \sum_{m,n,p} \frac{\langle g | \mu_\alpha | m \rangle \langle m | \mu_\gamma | n \rangle \langle n | \mu_\delta | p \rangle \langle p | \mu_\beta | g \rangle}{(\Omega_{mg} - \omega)(\Omega_{ng} - \omega)(\Omega_{pg})} - \sum_{m,n} \frac{\langle g | \mu_\alpha | m \rangle \langle m | \mu_\gamma | g \rangle \langle g | \mu_\delta | n \rangle \langle n | \mu_\beta | g \rangle}{(\Omega_{mg} - \omega)(\Omega_{ng})(\Omega_{ng} + \omega)} \\ & \sum_{m,n,p}^{**} \frac{\langle g | \mu_\alpha | m \rangle \langle m | \mu_\delta | n \rangle \langle n | \mu_\beta | p \rangle \langle p | \mu_\gamma | g \rangle}{(\Omega_{mg} - \omega)(\Omega_{ng})(\Omega_{pg})} - \sum_{m,n}^{**} \frac{\langle g | \mu_\alpha | m \rangle \langle m | \mu_\delta | g \rangle \langle g | \mu_\beta | n \rangle \langle n | \mu_\gamma | g \rangle}{(\Omega_{mg} - \omega)(\Omega_{ng})(\Omega_{ng})} \\ & \sum_{m,n,p} \frac{\langle g | \mu_\alpha | m \rangle \langle m | \mu_\beta | n \rangle \langle n | \mu_\delta | p \rangle \langle p | \mu_\gamma | g \rangle}{(\Omega_{mg} - \omega)(\Omega_{ng} - \omega)(\Omega_{pg})} - \sum_{m,n} \frac{\langle g | \mu_\alpha | m \rangle \langle m | \mu_\beta | g \rangle \langle g | \mu_\delta | n \rangle \langle n | \mu_\gamma | g \rangle}{(\Omega_{mg} - \omega)(\Omega_{ng})(\Omega_{ng} + \omega)} \\ & \sum_{m,n,p} \frac{\langle g | \mu_\alpha | m \rangle \langle m | \mu_\beta | n \rangle \langle n | \mu_\gamma | p \rangle \langle p | \mu_\delta | g \rangle}{(\Omega_{mg} - \omega)(\Omega_{ng} - \omega)(\Omega_{pg} - \omega)} - \sum_{m,n} \frac{\langle g | \mu_\alpha | m \rangle \langle m | \mu_\beta | g \rangle \langle g | \mu_\gamma | n \rangle \langle n | \mu_\delta | g \rangle}{(\Omega_{mg} - \omega)(\Omega_{ng} - \omega)(\Omega_{ng})} \\ & \sum_{m,n,p} \frac{\langle g | \mu_\alpha | m \rangle \langle m | \mu_\gamma | n \rangle \langle n | \mu_\beta | p \rangle \langle p | \mu_\delta | g \rangle}{(\Omega_{mg} - \omega)(\Omega_{ng} - \omega)(\Omega_{pg} - \omega)} - \sum_{m,n} \frac{\langle g | \mu_\alpha | m \rangle \langle m | \mu_\gamma | g \rangle \langle g | \mu_\beta | n \rangle \langle n | \mu_\delta | g \rangle}{(\Omega_{mg} - \omega)(\Omega_{ng} - \omega)(\Omega_{ng})} \\ & \sum_{m,n,p} \frac{\langle g | \mu_\beta | m \rangle \langle m | \mu_\delta | n \rangle \langle n | \mu_\gamma | p \rangle \langle p | \mu_\alpha | g \rangle}{(\Omega_{mg})(\Omega_{ng} + \omega)(\Omega_{pg} + \omega)} - \sum_{m,n}^{**} \frac{\langle g | \mu_\beta | m \rangle \langle m | \mu_\delta | g \rangle \langle g | \mu_\gamma | n \rangle \langle n | \mu_\alpha | g \rangle}{(\Omega_{mg})(\Omega_{ng} + \omega)(\Omega_{ng})} \\ & \sum_{m,n,p}^{**} \frac{\langle g | \mu_\beta | m \rangle \langle m | \mu_\gamma | n \rangle \langle n | \mu_\delta | p \rangle \langle p | \mu_\alpha | g \rangle}{(\Omega_{mg})(\Omega_{ng})(\Omega_{pg} + \omega)} - \sum_{m,n} \frac{\langle g | \mu_\beta | m \rangle \langle m | \mu_\gamma | g \rangle \langle g | \mu_\delta | n \rangle \langle n | \mu_\alpha | g \rangle}{(\Omega_{mg})(\Omega_{ng} + \omega)(\Omega_{ng} + \omega)} \\ & \sum_{m,n,p}^{**} \frac{\langle g | \mu_\beta | m \rangle \langle m | \mu_\delta | n \rangle \langle n | \mu_\alpha | p \rangle \langle p | \mu_\gamma | g \rangle}{(\Omega_{mg})(\Omega_{ng} + \omega)(\Omega_{pg})} - \sum_{m,n}^{**} \frac{\langle g | \mu_\beta | m \rangle \langle m | \mu_\delta | g \rangle \langle g | \mu_\alpha | n \rangle \langle n | \mu_\gamma | g \rangle}{(\Omega_{mg})(\Omega_{ng})(\Omega_{ng} - \omega)} \\ & \sum_{m,n,p}^{**} \frac{\langle g | \mu_\beta | m \rangle \langle m | \mu_\alpha | n \rangle \langle n | \mu_\delta | p \rangle \langle p | \mu_\gamma | g \rangle}{(\Omega_{mg})(\Omega_{ng} - \omega)(\Omega_{pg})} - \sum_{m,n}^{**} \frac{\langle g | \mu_\beta | m \rangle \langle m | \mu_\alpha | g \rangle \langle g | \mu_\delta | n \rangle \langle n | \mu_\gamma | g \rangle}{(\Omega_{mg})(\Omega_{ng})(\Omega_{ng} + \omega)} \end{aligned}$$



These terms are expected to be greatly enhanced over all other terms and therefore dominate the expression for  $\gamma_{\text{Kerr}}^{\text{V}}$ . Retaining only the doubly enhanced terms results in the following expressions for the relevant tensor components of  $\gamma_{\text{Kerr}}^{\text{V}}$ :

$$\gamma_{\alpha\beta\beta\alpha}^{\text{V},\alpha}(-\omega;0,0,\omega) = 2\hbar^{-2} \left\{ \sum'_m \sum'_n \frac{2\alpha_{gm}^{\alpha\alpha} \mu_{mn}^{\beta} \mu_{ng}^{\beta} + \mu_{gm}^{\beta} \alpha_{mn}^{\alpha\alpha} \mu_{ng}^{\beta}}{\Omega_{mg} \Omega_{ng}} - \sum'_m \frac{\alpha_{gg}^{\alpha\alpha} \mu_{gm}^{\beta} \mu_{mg}^{\beta}}{\Omega_{mg} \Omega_{mg}} \right\}$$

(2.4.3a)

and  $\gamma_{\alpha\beta\alpha\beta}^{\text{V},\alpha}(-\omega;0,0,\omega) = \gamma_{\alpha\alpha\beta\beta}^{\text{V},\alpha}(-\omega;0,0,\omega)$

$$= \hbar^{-2} \left\{ \sum'_m \sum'_n \frac{2\alpha_{gm}^{\alpha\beta} \mu_{mn}^{\beta} \mu_{ng}^{\alpha} + 2\alpha_{gm}^{\beta\alpha} \mu_{mn}^{\alpha} \mu_{ng}^{\beta}}{\Omega_{mg} \Omega_{ng}} + \sum'_m \sum'_n \frac{\mu_{gm}^{\alpha} \alpha_{mn}^{\beta\alpha} \mu_{ng}^{\beta} + \mu_{gm}^{\beta} \alpha_{mn}^{\alpha\beta} \mu_{ng}^{\alpha}}{\Omega_{mg} \Omega_{ng}} - \sum'_m \frac{2\alpha_{gg}^{\alpha\beta} \mu_{gm}^{\alpha} \mu_{mg}^{\beta}}{\Omega_{mg} \Omega_{mg}} \right\}$$

(2.4.3b)

where

$$\alpha_{mn}^{\alpha\beta} = \hbar^{-1} \sum'_p \langle m | \mu_{\alpha} | p \rangle \langle p | \mu_{\beta} | n \rangle \frac{2\Omega_{pg}}{\Omega^2 - \omega^2} \quad (2.4.4)$$

is the Raman transition polarizability.

The dc Kerr effect birefringence measured in the laboratory is related to the isotropically averaged molecular hyperpolarizability tensor through the definition

$$\gamma_{\text{Kerr}} = 3/2 [ \langle \gamma \rangle_{\text{XXXX}} - \langle \gamma \rangle_{\text{XYYX}} ] , \quad (2.4.5)$$

where the notation is the same as in the calculations for  $\gamma_{\text{THG}}^{\text{V}}$  and  $\gamma_{\text{ESHG}}^{\text{V}}$ . Substituting Eqs.(2.4.3a, b) into Eqs.(2.3.6a, b) and Eq.(2.4.5), and recalling that

$$\mu_{\text{gm}}^{\text{x}} = \mu_{\text{gm}}^{\text{y}} , \quad \alpha_{\text{gg}}^{\text{xy}} = 0$$

and

$$\alpha_{\text{gm}}^{\text{xy}} = \alpha_{\text{gm}}^{\text{yx}} ,$$

one obtains the following expression for  $\gamma_{\text{Kerr}}^{\text{V}}$  of  $\text{CF}_4$ :

$$\gamma_{\text{Kerr}}^{\text{V},\alpha} = \frac{18}{5} \hbar^{-2} \sum_m' \sum_n' \frac{2 \alpha_{\text{gm}}^{\text{xy}} \mu_{\text{mn}}^{\text{y}} \mu_{\text{ng}}^{\text{x}} + \mu_{\text{gm}}^{\text{x}} \alpha_{\text{mn}}^{\text{xy}} \mu_{\text{ng}}^{\text{y}}}{\Omega_{\text{mg}} \Omega_{\text{ng}}} .$$

(2.4.6)

If one carefully retains the terms with only one of the factors  $(\Omega_{\text{V}} - \omega')$  in the denominator having  $\omega' = 0$ , as well as the doubly enhanced terms which gave rise to Eq.(2.4.6), one obtains the following additional contribution to  $\gamma_{\text{Kerr}}^{\text{V}}$  which involves the hyper-Raman  $\beta$ :

$$\gamma_{\text{Kerr}}^{\nu, \beta} = \frac{4}{15} \hbar^{-1} \sum_m \frac{2 \mu_{gm}^x (\beta_{xxx} + \beta_{xyy} + \beta_{zzx})_{mg} + \mu_{gm}^z (\beta_{xyy} + \beta_{zzx})_{mg}}{\Omega_{mg}}$$

(2.4.7)

The relations of Eq.(2.4.4) have been employed in obtaining this result.

The expressions given in Eqs.(2.3.8, 2.4.6, 2.4.7) allow one to calculate  $\gamma^{\nu}$  for ESHG and the dc Kerr effect.

The nature of the final expressions for  $\gamma^{\nu}$  and the manner in which they were derived may be clarified by reference to Fig.(2.1). The terms of Eq.(2.1.1) have been classified in Fig.(2.1) according to possible sequences of the vibrationally or electronically excited intermediate states  $|m\rangle$ ,  $|n\rangle$  and  $|p\rangle$  in the terms which contribute to  $\gamma^{\nu}$ . Making use of Eqs.(2.3.5, 2.4.4) allows sequences of electronic transition dipoles in Fig.(2.1a) to be collapsed into vibrational transition polarizabilities and hyperpolarizabilities as shown in Fig.(2.1b). Eqs.(2.3.8, 2.4.6, 2.4.7) result when the calculation is done with due regard for spatial subscripts in the numerator and frequency arguments in the denominator; account is taken of molecular symmetry, and the microscopic molecular result is isotropically averaged. The numerical evaluation will be

given in chapter 5. It may be noted that the various diagrams in Fig.(2.1) do not contribute equally to  $\gamma^V$ , and the allowed terms in the calculation will depend on the particular molecule. For  $\text{CF}_4$  all terms are allowed, but the  $\mu\mu\alpha$  and  $\mu\alpha\mu$  and  $\mu\beta$  terms are dominant for the nonlinear optical processes that we have considered.

Figure 2.1

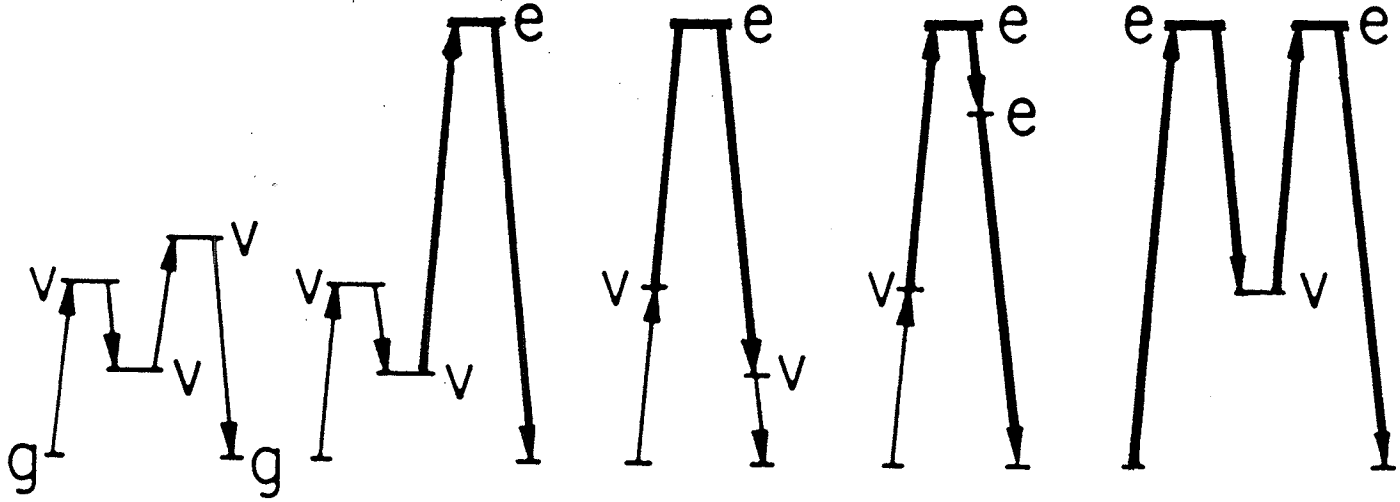
Diagrams for the five essential types of terms which contribute to  $\gamma^v$ .

(a). The arrows denote transition dipole matrix elements between states of the molecule. The states are labeled  $v$  or  $e$  according to whether they are vibrationally or electronically excited. All diagrams start and end at the molecular ground state  $g$ . Heavier arrows are drawn for electronic transitions.

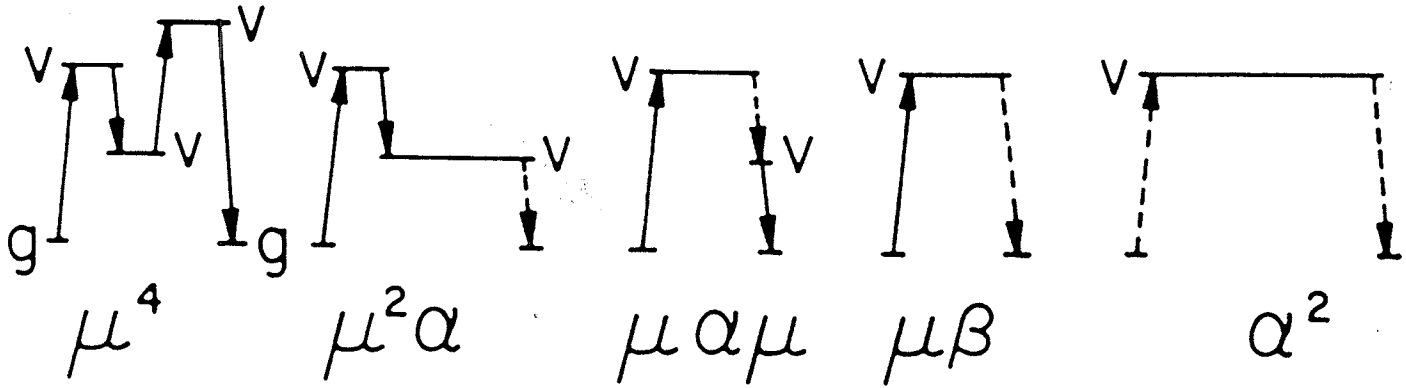
(b). Summing over the sequences of electronic transitions in (a) gives diagrams involving transition matrix elements of the Raman or hyper-Raman polarizabilities  $\alpha$  or  $\beta$  (dashed arrows). Thus, the diagrams for  $\gamma^v$  may be expressed in terms of vibrational transitions only, at the expense of containing matrix elements for all lower order processes.



a



b



### CHAPTER 3

#### EXPERIMENT

The experimental technique employed in this work is that of dc ESHG. This process was observed in gases, liquids and solids with high-power pulsed lasers during the 1960's and 1970's.<sup>1-4</sup> The technique of periodic phase matching, developed by D.P. Shelton and A.D. Buckingham at the beginning of the 1980's, allowed measurements to be made with a gas sample excited by a low-power laser beam.<sup>16</sup> The theory relating to this dc ESHG experiment has been well described in Refs.(10,16,17).

#### 3.1...Experimental System For dc ESHG

The basic idea in a dc ESHG experiment is to make measurements of the ratios of hyperpolarizabilities for the sample molecules against the reference molecules. As long as one knows the hyperpolarizability of the reference molecules, one obtains the hyperpolarizability of the sample molecules. In this experiment, the optical-field and static-field polarizations are parallel, so the measurements

are related to the XXXX component of the orientationally averaged tensor  $\gamma_{\alpha\beta\delta\gamma}$ . The ratio of hyperpolarizabilities for a sample gas B and a reference gas A is obtained from

$$\gamma_B/\gamma_A = (S_B^{(2\omega)}/S_A^{(2\omega)})^{1/2} (\rho_B n'_B / \rho_A n'_A)^{-1}, \quad (3.1.1)$$

where  $S^{(2\omega)}$  is the peak signal of the second harmonic,  $\rho$  is the number density and  $n'$  is defined by

$$n' = \{ (n_0^2+2)/3 \} \{ (n_\omega^2+2)/3 \}^2 \{ (n_{2\omega}^2+2)/3 \} / n_\omega^2 n_{2\omega}. \quad (3.1.2)$$

A schematic diagram of the optical system and the detection system is shown in Fig.(3.1). The fundamental CW light beam from a Rhodamine-6G or DCM dye laser (COHERENT CR-599 Dye Laser) pumped by an argon-ion laser (COHERENT CR-6 Innova Plasma Tube Ion Laser), or from the argon-ion laser directly, is redirected by plane mirrors. Then a well defined horizontal linear polarization state of the laser beam is selected by a Glan-laser prism polarizer. A filter is used to eliminate the unwanted second-harmonic light generated in the birefringent filter of the dye laser (The wavelength selector of the dye laser is a low-loss crystalline-quartz birefringent filter inserted in the three-mirror cavity.). The power of the laser beam is usually around 0.6-0.8 W at one of seven different wavelengths. The wavelengths of the laser beam from the dye laser are calibrated by Na or Ne atomic emission lines using spectral

lamps and a Jarrell-Ash 1m spectrometer. The laser beam is weakly focused, with a confocal parameter of about 20 cm, at the center of the gas cell to satisfy the requirement that the laser beam pass unobstructed through the long and narrow gap between the electrodes of the sample cell.

The sample gas cell is a cylinder with two optical windows supported on optically flat mounts at normal incidence to the beam. Inside the cell, there is a periodic electrode array in which a frequency-doubled beam is produced by passing a laser beam through the gas sample. The electrode array consists of 150 pairs of steel wires of 1.59 mm diameter and at a 2.69 mm center-to-center spacing. The length of the array is about twice the confocal parameter of the focused laser beam. Details of the construction of the electrode array can be found in Ref.(19). In this experiment the applied field is typically about 1.8 kV/mm. The gas cell is constructed to withstand high pressure. However in these experiments the pressure of the sample gas varies in the range of 2-6 atm. The pressure of gas is measured by a capacitance manometer (MKS Baratron) calibrated by the manufacturers and with a stated accuracy of 0.15%. The temperature is monitored inside the cell by a thermistor in direct contact with the gas, with accuracy

$\pm 0.2$  K.

After transmission through the sample cell, the laser beam is recollimated and sent through a double prism monochromator which eliminates most of the visible fundamental while passing the ultraviolet second harmonic signal. The Brewster angle dispersing prisms pass light polarized in the horizontal plane with negligible attenuation. A final filter (SCHOTT UG-5 OR CORNING CS7-54) eliminates the residual fundamental. The second-harmonic signal is detected by a photon counter with an uncooled EMI model No.9893QB/350 photomultiplier tube. The background in this experiment is usually about 0.5 cps, while the peak signal of the second-harmonic is around several hundred cps.

### 3.2 ... Sample Preparation And Effect Of Impurities

In this study,  $\text{CF}_4$  is the sample while  $\text{N}_2$  is the reference gas. Both gases are taken from Matheson. The purity of the  $\text{N}_2$  gas is 99.999% while that of the  $\text{CF}_4$  is better than 99.9%. A Ramam spectroscopic assay of the sample gas has been done in this laboratory using the  $\text{Ar}^+$

laser ( $\lambda=514.5$  nm) and a Jarrell-Ash 1m spectrometer. From the standard theory, the concentration of the impurity can be calculated from the following equation:

$$\rho_i/\rho_s = \frac{(I_i/I_s)(d\sigma/d\Omega)_s/(d\sigma/d\Omega)_{Q,N}}{(d\sigma/d\Omega)_i/(d\sigma/d\Omega)_{Q,N}} \quad (3.2.1)$$

where  $I$  is the peak signal in the Raman spectrum measured in the laboratory, and  $(d\sigma/d\Omega)$  is differential cross section. The subscripts "i" and "s" used in Eq.(3.2.1) denote "impurity" and "sample" respectively. Here "sample" refers to  $CF_4$ . A tabulation of  $(d\sigma/d\Omega)_i/(d\sigma/d\Omega)_{Q,N_2}$  can be found in Ref.(26). The calculation shows that the impurity of the  $CF_4$  sample gas is less than 0.058%:

$$CF_3Cl < 0.021\%$$

$$CHF_3 < 0.005\%$$

$$N_2 < 0.018\%$$

$$O_2 < 0.012\%$$

$$H_2O < 0.0018\%$$

Using the published measurements<sup>27, 28</sup> of the refractive index dispersion and the third-order susceptibility, and adding the contributions to the third-order susceptibility due to each of the impurities, one may estimate that the effect of the impurities will be to shift the measured

hyperpolarizability by less than 0.1% compared to that of pure  $\text{CF}_4$ . This effect is smaller than the accuracy of the ratio determination in this experiment.

### 3.3 ... Signal Curve and Data Analysis

The second-harmonic signal varies with the coherence length of the gas. The peak signal occurs when the coherence length of the gas matches the fixed spacing of the electrodes. The coherence length is adjusted by varying the gas pressure which is related to the gas density. Typical normalized experimental data of  $S$  against  $P$  are shown in Fig.(3.2), where  $S$  is the normalized strength of second-harmonic signal and  $P$  is the normalized pressure of gas. Using least squares fitting of a polynomial

$$S = \sum_n A_n P^n$$

to the measurements of  $S$  versus  $P$ , one finds that the data are very well represented regardless of taking the maximum power of  $n$  as  $N = 2, 3$  or  $4$ , provided only data taken symmetrically within about 10% of the peak signal are included. The difference in the peak values obtained with

fitting polynomials with  $N = 2, 3$  or  $4$  is only  $10^{-6}$  for  $\Delta S_{\text{peak}}$  and  $10^{-5}$  for  $\Delta P_{\text{peak}}$ . Based on this analysis, we simply choose a quadratic to fit the data taken symmetrically within around 10% of the peak. This provides a method to accurately determine the peak signal and the optimum pressure while avoiding fitting errors.

Measurements were made in coupled triplets (ABABA...) in order to cancel drifts. The sample densities were computed from the measured pressures and temperatures by iteratively solving the virial equation of state:

$$\rho_{n+1} = P / RT(1 + B\rho_n + C\rho_n^2) \quad (3.3.1)$$

where  $P$  is the pressure of the gas,  $T$  is the temperature,  $R$  is the universal gas constant and  $B$  and  $C$  are the second and third virial coefficients, respectively. Experimental virial coefficients for different real gases at different temperatures can be found in Ref.(29). In this experiment, the temperature is around 293 K, so we take

$$B = -4.46 \text{ cm}^3/\text{mole}, \quad C = 1063 \text{ cm}^6/\text{mole}^2 \quad (3.3.2)$$

for  $N_2$  gas and

$$B = -88.5 \text{ cm}^3/\text{mole}, \quad C = 6100 \text{ cm}^6/\text{mole}^2 \quad (3.3.3)$$

for  $CF_4$ . The density  $\rho$  usually converges with five iterations or less. Details of the computer programs are presented in the Appendix.



The estimated total experimental uncertainty of a hyperpolarizability-ratio measurement is obtained by convolving the statistical uncertainty for an average of usually five triplets of runs with the uncertainty of the density determinations due to the limited accuracy of the pressure gauge. The accuracy of the ratio determined in this experiment is estimated to be about 0.4%.

Figure 3.1

Experimental system

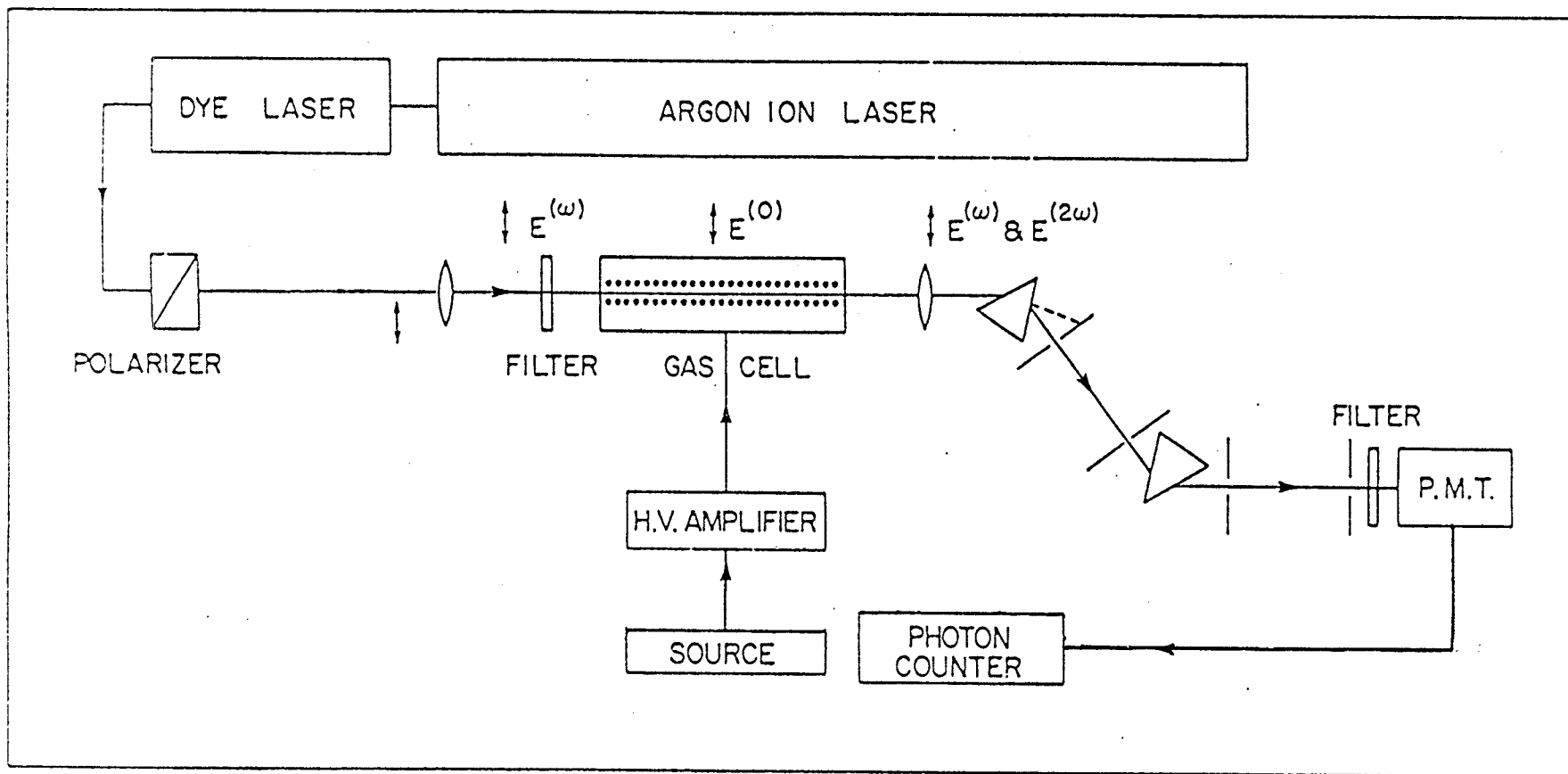
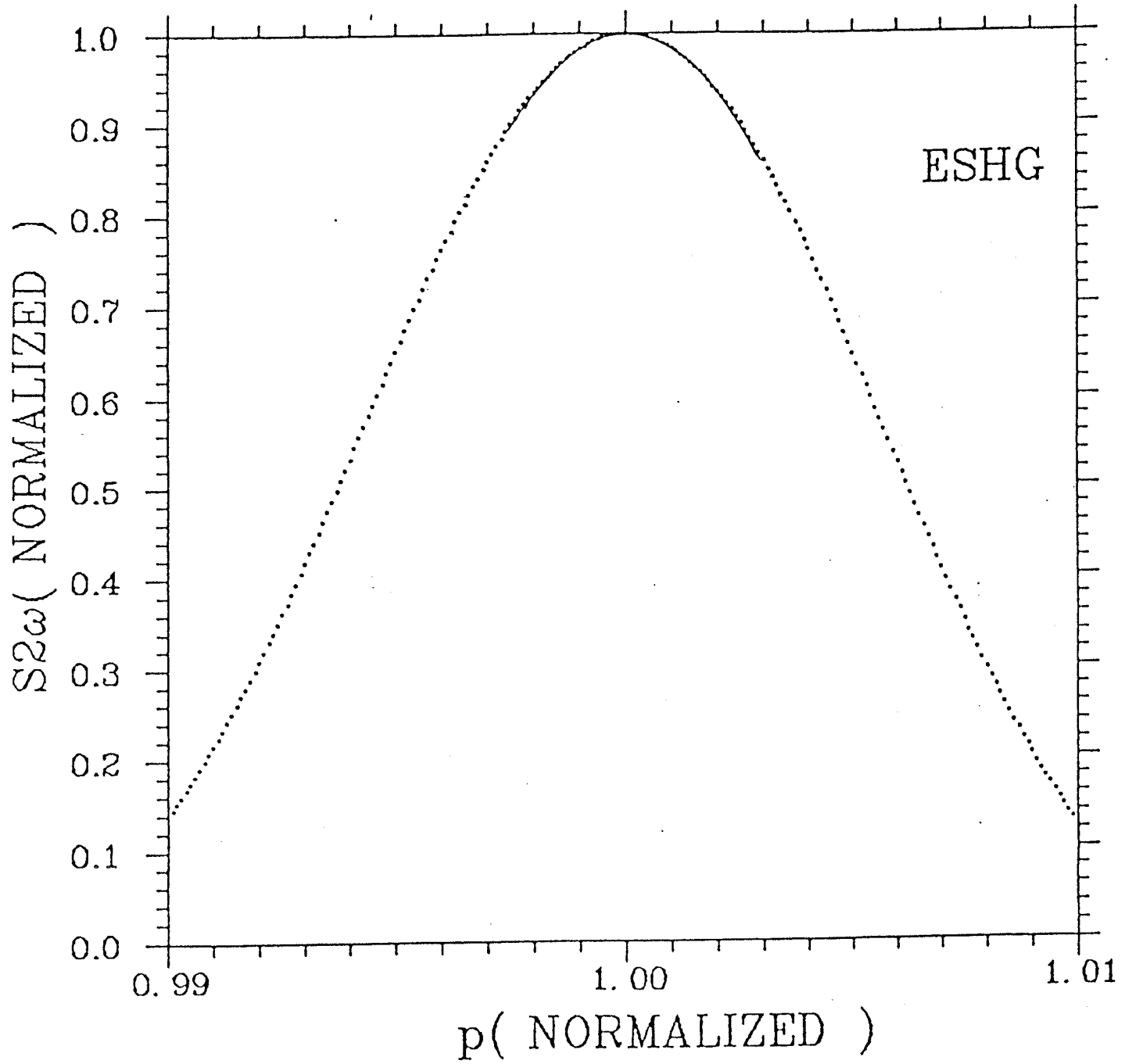


Figure 3.2

## Signal Curve And Least Squares Fitting Polynomial

In this figure, points denote experimental data and the solid line denotes the quadratic curve fitted to the data taken symmetrically within about 10% of the peak signal. In this case,  $\chi^2 \approx 0.001$ .



## CHAPTER 4

## EXPERIMENTAL RESULTS

The experiment gives the ratio of the peak signal for  $\text{CF}_4$  and  $\text{N}_2$ . To obtain the ratio of the hyperpolarizabilities, one needs to apply a local field correction factor. In this chapter, first we will calculate the local field correction factor and then give the second hyperpolarizability of  $\text{CF}_4$  from this experiment.

## 4.1 ... Local Field Correction Factor

The ratio  $\gamma_{\text{CF}_4} / \gamma_{\text{N}_2}$  can be obtained by using Eq.(3.1.1) and Eq.(3.1.2). Eq.(3.1.2) is

$$n' = [(n_0^2+2)/3] [(n_\omega^2+2)/3]^2 [(n_{2\omega}^2+2)/3] / n_\omega^2 n_{2\omega}$$

where  $n_0$  is the static refractive index of the gas,  $n_\omega$  is the refractive index of the gas at frequency  $\omega$  and  $n_{2\omega}$  is that at the doubled frequency, all evaluated at the gas density which gives phase matching. The final factor  $n_\omega^2 n_{2\omega}$  is not strictly a local field factor but it appears in the

expression for the ESHG signal. Taking  $n = 1 + \delta$  ( $\delta \ll 1$ ) and neglecting the higher orders of  $\delta$ , which is a good approximation in the experiment, one obtains a compact form for  $n'$  :

$$n' = (n_0^4 n_\omega^3 n_{2\omega})^{1/6}. \quad (4.1.1)$$

It is considered as a local field correction factor in obtaining the ratio  $\gamma_{CF_4} / \gamma_{N_2}$ . From the relation

$$n_\omega(T, P) - 1 = \alpha(\omega) \rho(T, P) / 2\epsilon_0 \quad (4.1.2a)$$

one may derive the following equation:

$$[n_\omega(T_2, P_2) - 1] = [n_\omega(T_1, P_1) - 1] \rho(T_2, P_2) / \rho(T_1, P_1), \quad (4.1.2b)$$

where  $T$  is the temperature of the gas and  $P$  the pressure. The mole density  $\rho(T_i, P_i)$  corresponds to  $n_\omega(T_i, P_i)$ . For  $N_2$ ,  $n_\omega$  and  $n_{2\omega}$  can be found from the tabulated values at standard conditions in Ref.(31) with linear interpolation to the seven frequencies corresponding to the ESHG experiment. For  $CF_4$ ,  $n_\omega$  can also be found in the same way, but  $n_{2\omega}$  is not available in the table.

To obtain  $n_{2\omega}$  for  $CF_4$ , one may use Eq.(4.1.2a) together with

$$\alpha(2\omega) = \alpha(\omega) + \Delta\alpha(\omega) \quad (4.1.3)$$

where

$$\Delta\alpha(\omega) = \alpha(2\omega) - \alpha(\omega) \quad (4.1.4)$$

is the linear polarizability dispersion. Applying Eq.(4.1.2a) for  $n_{2\omega}$ , one may write

$$n_{2\omega}(T,P) - 1 = \alpha(2\omega) \rho(T,P)/2\epsilon_0 . \quad (4.1.5)$$

From Eq.(4.1.5) and Eq.(4.1.2a), one gets

$$[n_{2\omega}(T,P) - 1] - [n_{\omega}(T,P) - 1] = \Delta\alpha \rho(T,P)/2\epsilon_0 . \quad (4.1.6)$$

It can be expressed in an alternative way when using Eq.(4.1.2a):

$$n_{2\omega}(T,P) - n_{\omega}(T,P) = \Delta\alpha [n_{\omega}(T,P) - 1]/\alpha(\omega) . \quad (4.1.7)$$

Let  $\rho(T_1, P_1)$  denote the mole density measured for  $n_{\omega}$  in Ref.(31) and  $\rho(T_2, P_2)$  denote the phase-matching density in our ESHG experiment. Substituting Eq.(4.1.2b) in Eq.(4.1.7), one obtains

$$n_{2\omega}(T_2, P_2) = n_{\omega}(T_2, P_2) + \Delta\alpha \{n_{\omega}(T_1, P_1) - 1\} \frac{\rho(T_2, P_2)}{\rho(T_1, P_1)\alpha(\omega)}$$

$$(4.1.8)$$

It is adequate to simply use the value given in Refs.(8, 31) for  $\lambda = 632.8$  nm,

$$\alpha(\omega) = 3.172 \times 10^{-4} \text{ C}^2 \text{ m}^2 \text{ J}^{-1}, \quad (4.1.9)$$

and

$$n_{\omega}(T_1, P_1) - 1 = 451.242 \times 10^{-6}, \quad (4.1.10)$$

to calculate  $n_{2\omega}$ . Finally,

$$n_{2\omega} = n_{\omega} + 1.423 \times 10^{36} \Delta\alpha(\omega) \rho(T_2, P_2) / \rho(T_1, P_1) . \quad (4.1.11)$$

To apply Eq.(4.1.11) to calculate  $n_{2\omega}$  for  $\text{CF}_4$ , one needs



$\Delta\alpha(\text{CF}_4)$ . However, in the ESHG experiment the wave-vector mismatch  $\Delta K$  is determined by the difference in the refractive index of the sample between  $\omega$  and  $2\omega$  expressed by

$$\begin{aligned}\Delta K &= 2K_\omega - K_{2\omega} = 4\pi(n_\omega - n_{2\omega})/\lambda_\omega \\ &= -\frac{2\pi}{\lambda_\omega \epsilon_0} (\Delta\alpha)\rho(T,P) + o(\rho^2) \quad . \quad (4.1.12)\end{aligned}$$

This implies that at the phase-matching case,

$$\text{i.e.} \quad \Delta K = \text{constant} ,$$

one can obtain the linear polarizability dispersion ratio by

$$\Delta\alpha_{\text{CF}_4} / \Delta\alpha_{\text{N}_2} = \rho_{\text{N}_2} / \rho_{\text{CF}_4} \quad (4.1.13)$$

using phase-matching densities measured in the ESHG experiment. Further, employing the measured values of  $\Delta\alpha_{\text{N}_2}$  in Ref.(30) at the corresponding frequencies one can obtain  $\Delta\alpha_{\text{CF}_4}$  from Eq.(4.1.13), and then  $n_{2\omega}$  can be calculated from Eq.(4.1.11).

For the static refractive index, from Eq.(4.1.2a) one obtains

$$n_0 - 1 = \alpha(0)\rho/2\epsilon_0 \quad (4.1.14)$$

Employing the published data in Refs.(32, 33):

$$\alpha_{\text{CF}_4}(0) = 4.270 \times 10^{-4} \text{C}^2 \text{m}^2 \text{J}^{-1} \quad (4.1.15)$$

$$\alpha_{\text{N}_2}(0) = 1.935 \times 10^{-4} \text{C}^2 \text{m}^2 \text{J}^{-1} \quad (4.1.16)$$

one gets

$$n_0(\text{CF}_4) = 1 + (1.452 \times 10^{-5} \text{m}^3/\text{mole}) \rho(T_2, P_2) \quad (4.1.17)$$

and

$$n_0(N_2) = 1 + (6.580 \times 10^{-6} \text{ m}^3/\text{mole}) \rho(T_2, P_2) . \quad (4.1.18)$$

The local field correction parameters have been listed with  $\Delta\alpha_{CF_4}$  in Table (4.1). They are seen to result in very small corrections, within the range of 0.05% to 0.17%.

#### 4.2 ... Dispersion of The Second Hyperpolarizability of $CF_4$ From ESHG Experiment

The results for ratios  $\gamma_{CF_4}/\gamma_{N_2}$  measured at seven wavelengths in the experiment are given in Table (4.2). To obtain  $\gamma_{CF_4}$  from the measured ratios, we have employed the previous measurements of  $\gamma_{N_2}/\gamma_{He}$  in Ref.(18) and the ab initio results for  $\gamma_{He}$  for calibration. The ab initio results for  $\gamma_{He}^{34}$  were calculated by Sitz and Yaris in 1968. Over the range of frequencies employed in the present measurements, these results are adequately represented by

$$\gamma_{He} = 42.6 \text{ a.u. } [1 + (2.94 \times 10^{10} \text{ cm}^2)\nu^2] . \quad (4.2.1)$$

On the other hand, from the previous work of Ref.(35), the ratios  $\gamma_{N_2}/\gamma_{He}$  over the same frequency range can be well represented by

$$\gamma_{N_2}/\gamma_{He} = 20.30 [1 + (6.55 \times 10^{10} \text{ cm}^2)\nu^2] , \quad (4.2.2)$$

where  $\nu$  is given in  $\text{cm}^{-1}$  and  $1 \text{ a.u.} = 6.2360 \times 10^6 \text{ C}^4 \text{ m}^4 \text{ J}^{-3}$ . An uncertainty of  $\pm 0.4\%$  due to  $\gamma_{\text{N}_2}/\gamma_{\text{He}}$  calibration has been assumed in assigning the error bars for  $\gamma_{\text{CF}_4}$ . The ab initio result for  $\gamma_{\text{He}}$  are thought to be accurate to  $1\%$ .<sup>35</sup> No allowance has been made for the uncertainty of  $\gamma_{\text{He}}$  in arriving at the experimental results for  $\gamma_{\text{CF}_4}$  given in Table (4.2). The experimental results for  $\gamma_{\text{CF}_4}$  are plotted versus  $\nu^2$  in Fig.(4.1). They are adequately represented by a straight line. The previous results are also plotted in Fig.(4.1). These results are seen to be in good agreement with the present ESHG measurements for  $\gamma_{\text{CF}_4}$ .

Figure 4.1

The values of  $CF_4$  measured in the present ESHG experiments ( filled circles ) and in previous experiments ( open circles ) are plotted versus  $\nu^2$ . The straight line is a fit of the function

$$Y = A ( 1 + B\nu^2 )$$

to the data of the present experiments. The coefficients of the fit are

$$A = 60.03 \times 10^{-63} \text{ C}^4 \text{ m}^4 \text{ J}^{-3}$$

and

$$B = 7.93 \times 10^{-10} \text{ cm}^2,$$

where  $\nu$  is given in  $\text{cm}^{-1}$ .

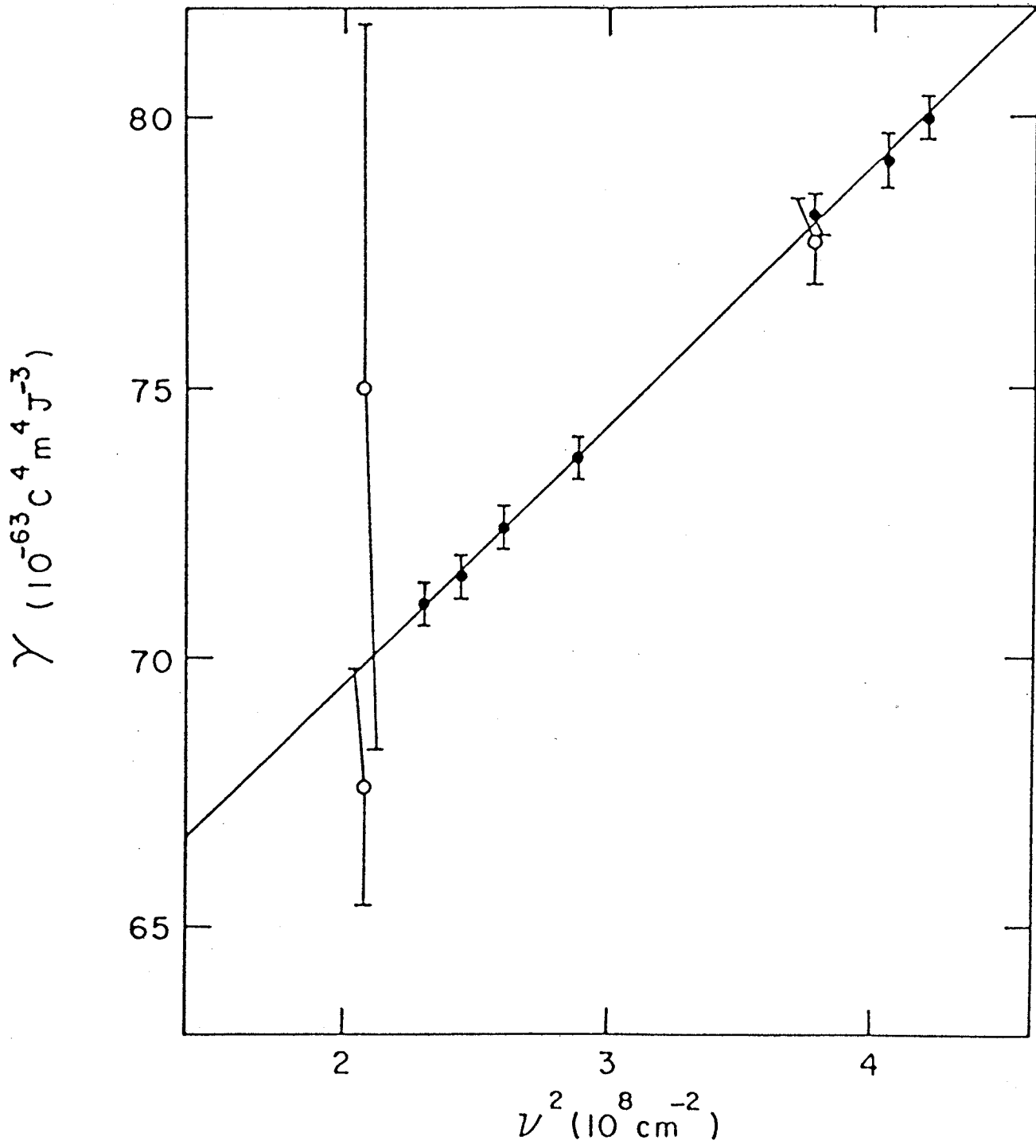


Table 4.1

Local field correction factor.

$\lambda$ (nm)	$\text{CF}_4$ ( $10^{41} \text{C}^2 \text{m}^2 \text{J}^{-1}$ )	$n^{\sim}(\text{CF}_4)$	$n^{\sim}(\text{N}_2)$	$n^{\sim}(\text{CF}_4)/n^{\sim}(\text{N}_2)$
488.0	1.498	1.001531	1.000785	1.00075
496.5	1.444	1.001612	1.000829	1.00078
514.5	1.339	1.001799	1.000930	1.00087
589.0	1.019	1.001984	1.001442	1.00054
621.7	0.9193	1.003186	1.001714	1.00147
640.2	0.8701	1.003468	1.001880	1.00158
659.8	0.8234	1.003777	1.002045	1.00173

Table 4.2

Experimental results for  $\Upsilon$  of  $\text{CF}_4$  measured by ESHG over the visible.

$\lambda$ (nm)	$\nu$ ( $\text{cm}^{-1}$ )	$\Upsilon_{\text{CF}_4} / \Upsilon_{\text{N}_2}$	$\Upsilon_{\text{CF}_4}$ ( $10^{-6} \text{ C}^4 \text{ m}^4 \text{ J}^{-3}$ )
488.0	20486	$1.036 \pm 0.003$	$80.0 \pm 0.4$
496.5	20135	$1.036 \pm 0.004$	$79.2 \pm 0.5$
514.5	19430	$1.046 \pm 0.003$	$78.2 \pm 0.4$
589.0	16973	$1.060 \pm 0.002$	$73.7 \pm 0.4$
621.7	16080	$1.068 \pm 0.004$	$72.4 \pm 0.4$
640.2	16615	$1.067 \pm 0.004$	$71.5 \pm 0.4$
659.8	15152	$1.072 \pm 0.004$	$71.0 \pm 0.4$

## CHAPTER 5

DISCUSSION:  $\gamma_{\text{THG}}^{\text{V}}$ ,  $\gamma_{\text{ESHG}}^{\text{V}}$  AND  $\gamma_{\text{Kerr}}^{\text{V}}$  FOR  $\text{CF}_4$ 

Our purpose in this work is to analyze the vibrational contributions to the second hyperpolarizability of  $\text{CF}_4$ . We have derived the expressions of  $\gamma^{\text{V}}$  for  $\text{CF}_4$  in different nonlinear processes and obtained the results for  $\gamma$  from an ESHG experiment. Next we will give a numerical estimation and discussion of  $\gamma_{\text{CF}_4}^{\text{V}}$ .

5.1 ...  $\gamma_{\text{THG}}^{\text{V}}$  And  $\gamma_{\text{ESHG}}^{\text{V}}$  For  $\text{CF}_4$ 5.1.1 ... Previous Results for  $\gamma_{\text{CF}_4}^{\text{V}}$  in THG, ESHG and the dc Kerr effect

Before proceeding with the numerical evaluation of  $\gamma^{\text{V}}$ , it is useful to compare the experimental measurements for several different third-order optical processes, ignoring for the moment the contribution due to  $\gamma^{\text{V}}$ . It has been suggested in Refs.(10, 36) that far below resonance the



electronic contributions to  $\gamma$  for the various third-order nonlinear optical processes will obey the relation

$$\gamma^e(\omega_\sigma; \omega_1, \omega_2, \omega_3) = \gamma(0; 0, 0, 0) \times (1 + C\omega_L^2) \quad (5.1.1)$$

where

$$\omega_L^2 = \omega_\sigma^2 + \omega_1^2 + \omega_2^2 + \omega_3^2 \quad (5.1.2)$$

is the effective laser frequency. If it is the case that the electronic contributions to  $\gamma_{CF_4}$  are dominant, the values of  $\gamma_{CF_4}$  experimentally determined by means of different nonlinear optical processes should all fall on the same straight line when plotted versus  $\nu_L^2$ .

The previously published values of  $\gamma_{CF_4}$  from the dc Kerr effect,<sup>37,38</sup> ESHG<sup>16,39,40</sup> and THG<sup>41</sup> experiments have been collected in Table (5.1) and have been plotted versus  $\nu_L^2$  in Fig.(5.1). The straight line drawn there is the least squares fit of Eq.(5.1.1) to the experimental ESHG results of the present work. Two discordant values of  $\gamma_{CF_4}$  from the dc Kerr effect experiments are given in Table (5.1), but only one has been plotted in Fig.(5.1). The earlier measurement in Ref.(37) was made on a sample of relatively low purity, only 98%, the chief impurity being air. One may estimate that the effect of 2% air as an impurity will be to increase the apparent value of  $\gamma_{CF_4}$  by 10%. A similar systematic error would arise from as little as 0.1% of typical fluoromethane

Table 5.1

Hyperpolarizability of  $\text{CF}_4$  previously measured by several nonlinear optical processes.

Process	$\lambda$ (nm)	$\chi_L^2$ ( $10^8 \text{ cm}^{-2}$ )	$\gamma_{\text{CF}_4}$ ( $10^{-6} \text{ C}^4 \text{ m}^4 \text{ J}^{-3}$ )
dc Kerr	632.8	4.99	$92.8 \pm 5.2^a$
	632.8	4.99	$77.0 \pm 6.0^b$
ESHG	694.3	12.45	$75.0 \pm 6.7^c$
	694.3	12.45	$67.6 \pm 2.2^d$
	514.5	22.66	$77.7 \pm 0.8^e$
THG	694.3	24.89	$73.5 \pm 3.7^f$

a. From Ref.(37)

b. From Ref.(38)

c. From Ref.(39)

d. From Ref.(40)

e. Recalculated from the result given in Ref.(16), using the more accurate value of  $\gamma_{\text{CH}_4}$  from Ref.(36) for calibration.

f. From Ref.(41)

impurities. The effect of impurities would be revealed by a spurious temperature dependence of the measured  $\gamma_{CF_4}$ , but the measurements of Ref.(37) were made at only a single temperature. The later measurement in Ref.(38), on the other hand, used a sample of much higher purity (99.7%) and demonstrated temperature independence of the measured value of  $\gamma_{CF_4}$  over the temperature range 269-322 K. On the basis of these considerations, we have rejected the result of Ref.(37) in favor of the result of Ref.(38), which alone has been plotted in Fig.(5.1). Comparing the dc Kerr and THG measurements with the straight line fitted to the ESHG measurements, one finds that the dc Kerr measurement falls about 20% above, while the THG measurement result falls about 7% below the straight line. These differences are well outside the error bars of the various measurements, which clearly indicates that there is a different balance of vibrational contributions for different processes.

#### 5.1.2 ... $\gamma_{THG}^V$ And $\gamma_{ESHG}^V$ For $CF_4$

To evaluate the vibrational contribution to  $\gamma_{THG}$  for

$CF_4$  using Eq.(2.2.7) derived in chapter 2, we employ the dipole matrix elements given in Table (5.2). These matrix elements for  $CF_4$  are obtained from experimental measurements of infrared absorption and Raman scattering using the standard theory. The sum

$$\sum_m' |\mu_{mg}^x| = 1.3 \times 10^{-6} \text{ C m}^2 \quad (5.1.3)$$

is dominated (95% contribution) by the  $\nu_3$  vibrational fundamental. Using the  $\nu_3$  vibrational transition frequency as  $\Omega_V$  in Eq.(2.2.7), one gets

$$\gamma_{THG}^V \approx 1.1 \times 10^{-6} \text{ }^3\text{C}^4 \text{ m}^4 \text{ J}^{-3} \quad (5.1.4)$$

This is only about 1% of the total  $\gamma$ . The accuracy of Eq.(5.1.4) may be difficult to assess, but even if it were in error by a factor of three,  $\gamma_{THG}^V$  would still be very small compared to  $\gamma^e$  for  $CF_4$ . It indicates that  $\gamma_{THG}^V$  is almost negligible in comparison to the electronic contribution, and suggests that the vibrationally corrected  $\gamma_{THG}$  may be used to calibrate the electronic contributions to the other processes for  $CF_4$ . Following this idea and taking  $\gamma_{ESHG}^V$  as the vertical distance between the ESHG line and the vibrationally corrected THG point, the vibrational contribution to  $\gamma_{ESHG}$  is estimated to be  $7.1 \times 10^{-6} \text{ }^3\text{C}^4 \text{ m}^4 \text{ J}^{-3}$ . It may be seen from Eq.(2.3.8) that there is a term of  $\gamma_{ESHG}^V$  which varies as  $\omega^{-3}$ . However, evaluating this term using the

matrix elements given in Table (5.2), one finds that it is only  $0.14 \times 10^{-6} \text{C}^4 \text{m}^4 \text{J}^{-3}$ . This is negligible. Therefore, at optical frequencies the vibrational contribution to  $\gamma_{\text{ESHG}}$  is nearly independent of  $\omega$ . Subtracting the value of  $\gamma_{\text{ESHG}}^{\text{v}}$  from the  $\gamma_{\text{ESHG}}$  data to obtain  $\gamma_{\text{ESHG}}^{\text{e}}$  only causes a parallel translation of the straight line shown in Fig.(5.1). The estimate of  $\gamma^{\text{e}}$  obtained by a parallel translation of the  $\gamma_{\text{ESHG}}$  line until it passes through the  $\gamma_{\text{THG}}^{\text{e}}$  point is shown as the dashed line in Fig.(5.1). Deviations of the measured values of  $\gamma$  from this dashed line are to be interpreted as vibrational contributions. If this analysis is correct,  $\gamma^{\text{v}}$  calculated from Eq.(2.3.8) for ESHG and Eqs.(2.4.6, 2.4.7) for the dc Kerr effect must agree with the experimental values which are obtained from Fig.(5.1).

Evaluation of  $\gamma_{\text{ESHG}}^{\text{v}}$  from Eq.(2.2.14) would be straight forward, except that there have been no measurements of the hyper-Raman  $\beta$  for  $\text{CF}_4$  that we need for our analysis. However, there have been measurements of the hyper-Raman spectra of various other  $\text{CX}_4$  compounds.<sup>42, 44</sup> Therefore, we will use the measurements<sup>43</sup> and calculations<sup>45</sup> which have been made for  $\text{CH}_4$  for guidance.

5.1.3 ...Hyper-Raman  $\beta$ 

The hyper-Raman spectrum of  $\text{CH}_4$  was recorded by Verdieck and Peterson in 1970.<sup>4,3</sup> The spectrum shows that the intensity of the hyper-Rayleigh line and the  $\nu_3$  Stokes hyper-Raman line are of the same order, and that all other transitions are much weaker. What the experiment measured is the XXX component of the isotropically averaged  $\beta^2$ , which may be expressed in terms of the hyperpolarizability components in the molecule fixed frame by the expression:<sup>2,3</sup>

$$\begin{aligned} \langle \beta^2 \rangle_{\text{XXX}} = (1/35) \{ & 5 \sum_{\alpha} \beta_{\alpha\alpha\alpha}^2 + 6 \sum_{\alpha \neq \beta} \beta_{\alpha\alpha\alpha} \beta_{\alpha\beta\beta} \\ & + 9 \sum_{\alpha \neq \beta} \beta_{\alpha\alpha\beta}^2 + 6 \sum_{\substack{\alpha, \beta, \gamma \\ \text{cyclic}}} \beta_{\alpha\alpha\beta} \beta_{\beta\gamma\gamma} + 12 \beta_{\alpha\beta\gamma}^2 \} \end{aligned}$$

(5.1.4)

Assuming that the hyper-Rayleigh and the Stokes hyper-Raman scattering have equal intensities, and that

$$\beta_{\text{xxx}} = \beta_{\text{xyy}} = \beta_{\text{zzx}} \quad (5.1.5)$$

is valid for a  $\text{CX}_4$  molecule, Eq.(5.1.4) may be applied to obtain the following relation between the magnitude of the hyper-Raman and hyper-Rayleigh hyperpolarizability components:

$$|\langle \beta \rangle_{\text{ZZZ}}|(\nu_3) \sim 1/3 |\langle \beta \rangle_{\text{XYZ}}|(\text{Rayleigh}). \quad (5.1.6)$$

Hyper-Rayleigh scattering by a tetrahedral molecule is mediated by the single nonvanishing hyperpolarizability component  $\beta_{xyz}$ , whose magnitude was estimated theoretically by Buckingham and Stephan to be  $7.8 \times 10^{-52} \text{C}^3 \text{m}^3 \text{J}^{-2}$  for  $\text{CH}_4$ . Hyper-Raman scattering is mediated by several components of the transition hyperpolarizability. Eq.(2.3.8) for  $\gamma_{\text{ESHG}}^{\text{V}}$  involves the following combination of transition hyperpolarizability components:

$$\beta_{\text{eff}} = \beta_{zzz} + \beta_{zxx} + \beta_{yyz}, \quad (5.1.7)$$

which may be evaluated by means of Eq.(5.1.5) to obtain

$$|\beta_{\text{eff}}| = |\beta_{xyz}| = 7.8 \times 10^{-52} \text{C}^3 \text{m}^3 \text{J}^{-2} \quad (5.1.8)$$

for  $\text{CH}_4$ . With this value of  $\beta_{\text{eff}}$ , and using the transition matrix elements given in Ref.(8), one obtains from Eq.(2.3.8) the estimate

$$\gamma_{\text{ESHG}}^{\text{V}} = 3 \times 10^{-6} \text{C}^3 \text{m}^4 \text{J}^{-3} \quad (5.1.9)$$

for  $\text{CH}_4$ . This is only 1% of the total  $\gamma_{\text{ESHG}}$  of  $\text{CH}_4$ . In a similar fashion, using Eq.(2.3.8) and the matrix elements of Table (5.2) and the observed difference

$$\gamma_{\text{ESHG}} - \gamma_{\text{THG}}^{\text{e}} = 7.1 \times 10^{-6} \text{C}^3 \text{m}^4 \text{J}^{-3}, \quad (5.1.10)$$

one deduces

$$|\beta_{\text{eff}}| \approx 1.3 \times 10^{-52} \text{C}^3 \text{m}^3 \text{J}^{-2} \quad (5.1.11)$$

for the  $\nu_3$  mode of  $\text{CF}_4$ . One may note that this value is  $6 \times$  smaller than the corresponding value for  $\text{CH}_4$ .

## 5.2 ... $\gamma_{\text{Kerr}}^{\text{V}}$ for $\text{CF}_4$

### 5.2.1 ... The Nature of The Vibrations For $\text{CF}_4$

Before attempting to evaluate  $\gamma_{\text{Kerr}}^{\text{V}}$ , it is useful to consider in more detail the nature of the vibrations for  $\text{CF}_4$ . As a spherical top molecule,  $\text{CF}_4$  has fundamentals  $\nu_1$ ,  $\nu_2$ ,  $\nu_3$  and  $\nu_4$  with the symmetry assignments  $a_1$ , e,  $f_2$  and  $f_2$  in the  $T_d$  group respectively. The normal vibrations corresponding to  $\nu_1$ ,  $\nu_2$ ,  $\nu_3$  and  $\nu_4$  have been shown in Fig.(5.2). All of the four fundamentals are Raman active, while only  $\nu_3$  and  $\nu_4$  are infrared active. The symmetry of a combination or overtone level is obtained from the direct product of irreducible representations, and will be a sum of  $a_1$ ,  $a_2$ , e,  $f_1$  and  $f_2$  terms. The transitions with nonvanishing dipole matrix elements are just those for which the symmetry species  $f_2$  appear at least once in the direct product of the representations of the initial and final levels of the transition. The three degenerate components of a mode of  $f_2$  symmetry may taken as vibrations in the x,y and z directions, in which case only a single transition dipole matrix element and a single pair of transition polarizability matrix elements are nonvanishing for each vibrational component, as shown in Fig.(5.2). The



vibrational components and the corresponding nonvanishing matrix elements are

$$x: \quad \mu^x, \quad \alpha^{yz} = \alpha^{zy} \quad (5.2.1a)$$

$$y: \quad \mu^y, \quad \alpha^{zx} = \alpha^{xz} \quad (5.2.1b)$$

and

$$z: \quad \mu^z, \quad \alpha^{xy} = \alpha^{yx} \quad (5.2.1c)$$

The nonvanishing matrix elements also satisfy

$$\mu^x = \mu^y = \mu^z \quad (5.2.2a)$$

and

$$\alpha^{xy} = \alpha^{yz} = \alpha^{zx} \quad (5.2.2b)$$

Note that only vibrations of  $f_2$  symmetry contribute to the final expressions for  $\gamma_{\text{ESHG}}^V$  and  $\gamma_{\text{Kerr}}^V$ , Eqs.(2.3.8, 2.4.6, 2.4.7), and that the 3-fold degeneracy of such vibrations has already been accounted for by making use of Eq.(2.3.6) for the isotropic averages. However, when symmetry species  $f_2$  appears  $n$  times in the representation of a particular vibrational overtone or combination transition, then one must multiply the matrix element by an extra degeneracy factor  $n$ . Furthermore, in the harmonic approximation, the matrix element for the hot band transition  $v_i, v_j \rightarrow v_i, v_j+1$  is proportional to  $(v_j+1)$ . Such a simple result is not obtained for overtone and combination transitions, which are not allowed in the harmonic approximation. So for

simplicity we have assumed that an overtone or combination transition starting from an excited level has the same matrix element as the same transition starting from the ground state.

### 5.2.2 ... $\gamma_{\text{Kerr}}^{\text{V}}$ - Significant But Not Large

The evaluation of  $\gamma_{\text{Kerr}}^{\text{V}}$  from Eqs.(2.4.6) and (2.4.7) makes use of the matrix elements given in Table (5.2) and the hyper-Raman  $\beta$  deduced when considering  $\gamma_{\text{ESHG}}^{\text{V}}$ . Evaluation of Eq(2.4.6) is performed by writing out diagrams with three successive transitions  $g \rightarrow m \rightarrow n \rightarrow g$ , using matrix elements selected from Table (5.2). The number of diagrams used for calculation is about 100 altogether. Taking all the matrix elements to be positive when computing the diagrams, and noting that many of the required matrix elements correspond to hot band transitions, one obtains:

$$\gamma_{\text{Kerr}}^{\text{V},\alpha} = 20.2 \times 10^{-6} \text{ }^3\text{C}^4 \text{m}^4 \text{J}^{-3}. \quad (5.2.3)$$

When Eq.(2.4.7) is evaluated and added, the final result is:

$$\gamma_{\text{Kerr}}^{\text{V}} = 23.0 \times 10^{-6} \text{ }^3\text{C}^4 \text{m}^4 \text{J}^{-3}. \quad (5.2.4)$$

One sees that Eq.(2.4.7) involving the hyper-Raman  $\beta$  makes

only a small contribution to the total. Subtracting Eq. (5.2.4) from the measured value of  $\gamma_{\text{Kerr}}$  one obtains  $\gamma_{\text{Kerr}}^{\text{V}}$  which has been plotted as the open triangle in Fig.(5.1). The error bar of the plotted point overlaps the dashed line representing  $\gamma^e$ , just as required by our analysis.

The calculated value of  $\gamma_{\text{Kerr}}^{\text{V}}$  finally permits a clear test of our calculations of  $\gamma^{\text{V}}$ . We had proceeded by attributing the difference between the  $\gamma_{\text{THG}}^e$  and  $\gamma_{\text{ESHG}}$  measurements to  $\gamma_{\text{ESHG}}^{\text{V}}$ . However, the theoretical expression for  $\gamma_{\text{ESHG}}^{\text{V}}$  is proportional to the unknown hyper-Raman  $\beta$  for  $\text{CF}_4$ , so the calculation for  $\gamma_{\text{ESHG}}^{\text{V}}$  ends up being used to determine the free parameter  $\beta$ . For  $\gamma_{\text{Kerr}}^{\text{V}}$ , no further unknown parameters enter the calculation and so one may carry through the comparison of theory and experiment in order to judge the accuracy of the calculation. Thus, the fact that all the vibrationally corrected measurements fall on the same line seems to support the adequacy of our analysis. It should be noted, however, that the calculated  $\gamma_{\text{Kerr}}^{\text{V}}$  is likely to be an overestimate since all matrix elements were assumed to be positive in the evaluation of the theoretical expressions. One may expect that there will be a cancellation of terms if some matrix elements are negative, which may significantly reduce the calculated

value of  $\gamma_{\text{Kerr}}^{\text{v}}$ . Nevertheless, the numerical results obtained here are much more reliable than those previously obtained by Elliott and Ward in 1984.<sup>8</sup> Their calculation gave

$$\gamma_{\text{Kerr}}^{\text{v}} = 3\gamma^{\text{e}} ,$$

which is about  $10\times$  too large.

Figure 5.1

Experimental values of  $\gamma_{CF_4}$  measured by the dc Kerr effect (triangles), ESHG (circles) and THG (square) are plotted versus  $\nu_L^2$  (defined by Eq.(5.1.2)). The filled symbols are the directly measured values of  $\gamma$ , while the open symbols are the corresponding results after subtracting the calculated vibrational contributions to obtain the purely electronic contribution  $\gamma^e$ . Note that the vibrational contribution is very small for THG. In Fig. (5.1), the solid line is the straight line which was fit to the ESHG data, while the dashed line is the corresponding straight line fit to the vibrationally corrected ESHG data points. All the measurements of  $\gamma^e$  (open symbols) fall on the dashed straight line to within the error bars, as predicted by Eq.(5.1.1).

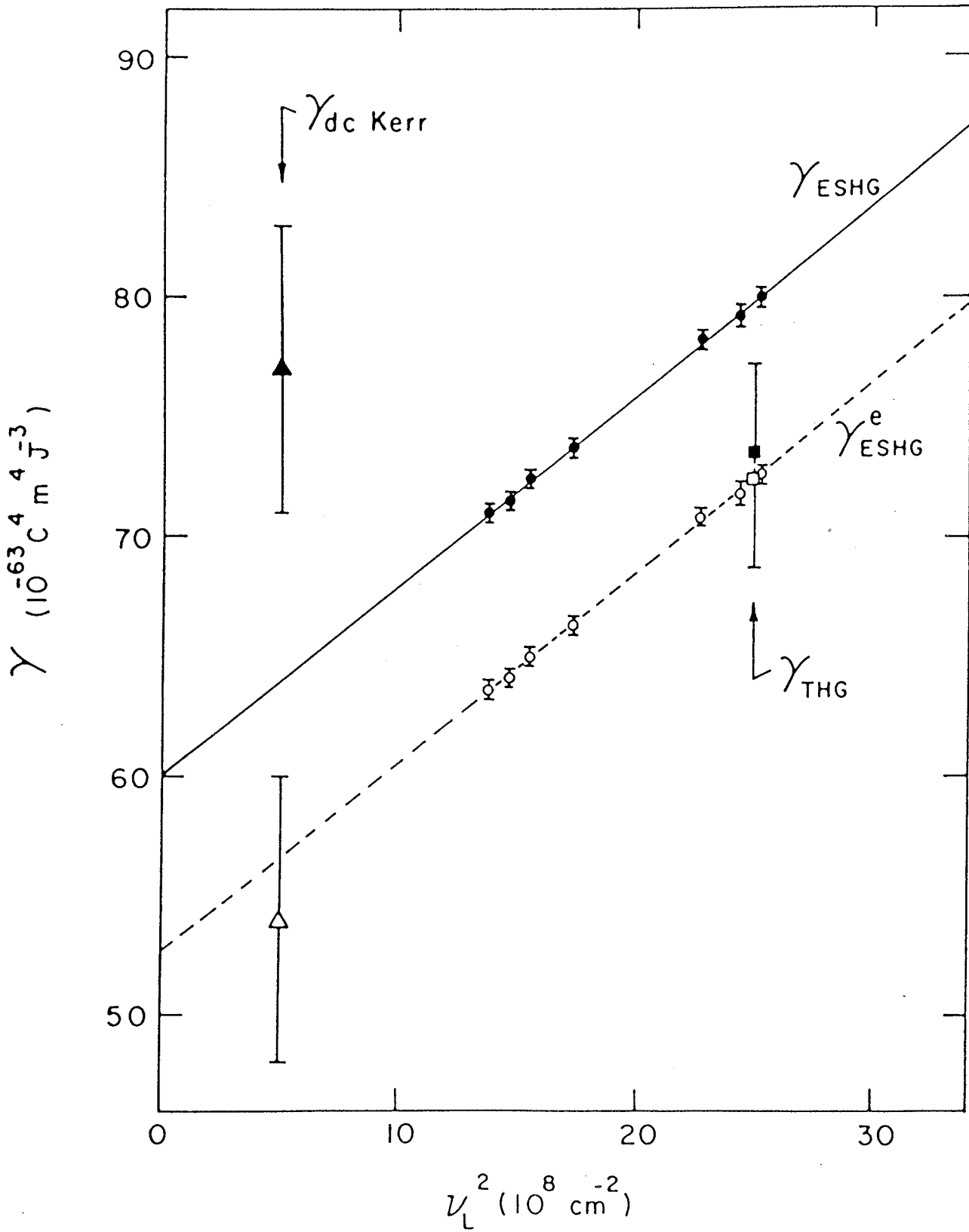
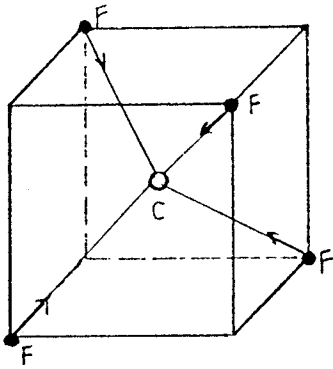
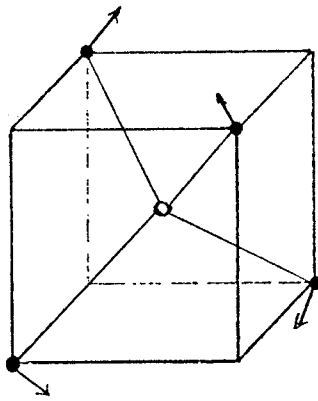


Figure 5.2

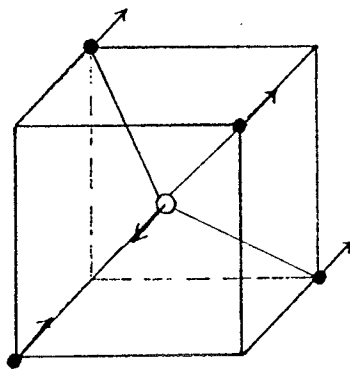
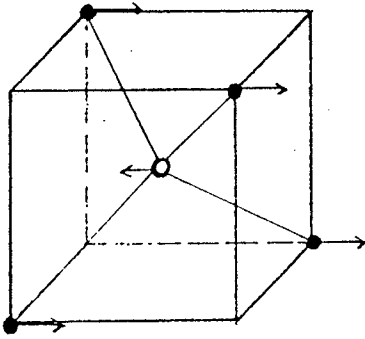
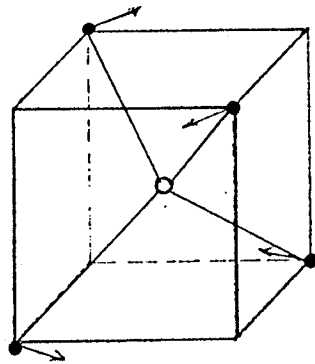
The normal vibrations with symmetry  $a_1$ ,  $e$ ,  $f_2$ , and  $f_2$   
of the molecule  $CF_4$ .<sup>46</sup>



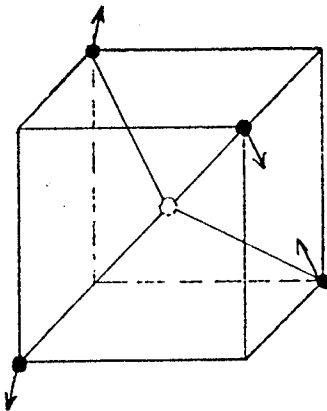
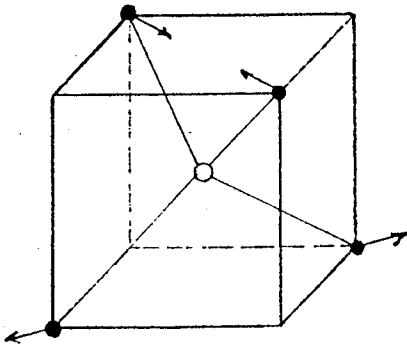
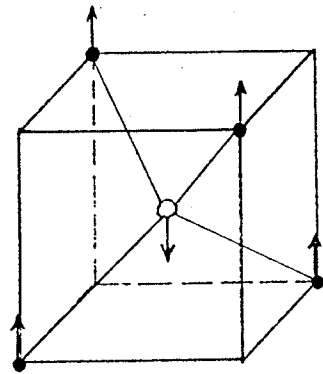
$A_1 (V_1)$



$E (V_2)$



$F_2 (V_3)$



$F_2 (V_4)$

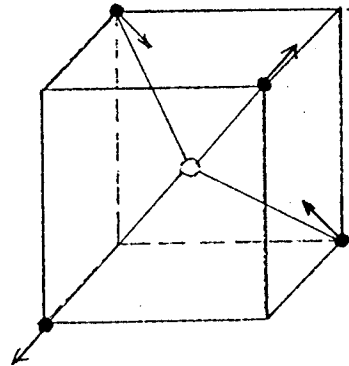




Table 5.2

Matrix elements for transitions from the ground state for the  $\text{CF}_4$  molecule. The symmetry species for the upper level of each transition are given in the column labeled species. The matrix elements have been deduced from infrared absorption and Raman scattering data as outlined in Refs.(8, 26, 46-49). The observables in a Raman scattering experiment are the mean polarizability and the anisotropy, usually denoted by "a" and " $\gamma$ ". Summing over degenerate modes, these may be written as

$$a = 1/3 (\alpha^{xx} + \alpha^{yy} + \alpha^{zz})$$

and

$$\gamma^2 = (\alpha^{xx} - \alpha^{yy})^2 + 9(\alpha^{xy})^2$$

in terms of the independent components of the transition polarizability tensor for  $\text{CF}_4$ .

Assign.	species	$\nu_{gm}$ ( $\text{cm}^{-1}$ )	$ \mu_{gm}^x ^a$ ( $10^{-32}$ C m)	$ \alpha_{gm}^{xy} ^b$ ( $10^{-42}$ C <sup>2</sup> m <sup>2</sup> J <sup>-1</sup> )
$\nu_1$	$a_1$	908	0.	0. <sup>c</sup>
$\nu_2$	$e$	435	0.	0. <sup>d</sup>
$\nu_3$	$f_2$	1283	112.0	2.20
$\nu_4$	$f_2$	631	16.0	2.43
$2\nu_2$	$a_1+e$	869	0.	0. <sup>e</sup>
$2\nu_3$	$a_1+e+f_2$	2566	7.66	0.04 <sup>f</sup>
$2\nu_4$	$a_1+e+f_2$	1264	7.98	0.21 <sup>g</sup>
$\nu_1+\nu_3$	$f_2$	2187	4.43	
$\nu_1+\nu_4$	$f_2$	1536	8.86	
$\nu_2+\nu_3$	$f_1+f_2$	1718	3.49	
$\nu_2+\nu_4$	$f_1+f_2$	1067	3.94	
$\nu_3+\nu_4$	$a_1+e+f_1+f_2$	1915	3.95	
$\nu_1+\nu_3+\nu_4$	$a_1+e f_1+f_2$	2819	1.12	

Assign.	species	$\nu_{gm}$ ( $\text{cm}^{-1}$ )	$\left  \mu_{gm}^x \right ^a$ ( $10^{-32} \text{ C m}$ )	$\left  \alpha_{gm}^{xy} \right ^b$ ( $10^{-42} \text{ C}^2 \text{ m}^2 \text{ J}^{-1}$ )
$3\nu_4$	$a_1 + f_1 + 2f_2$	1896	0.18	
$3\nu_3$	$a_1 + f_1 + 2f_2$	3850	0.48	
$\nu_1 + 3\nu_3$	$a_1 + f_1 + 2f_2$	4753	0.19	
$2\nu_3 + \nu_4$	$a_1 + e + 2f_1 + 3f_2$	3198	0.56	
$\nu_1 + 2\nu_3 + \nu_4$	$a_1 + e + 2f_1 + 3f_2$	4102	0.24	
$\nu_3 + 2\nu_4$	$a_1 + e + 2f_1 + 3f_2$	2547	5.10	
$\nu_1 + \nu_3 + 2\nu_4$	$a_1 + e + 2f_1 + 3f_2$	3450	0.69	
$2\nu_1 + \nu_3$	$f_2$	3091	0.61	
$2\nu_1 + \nu_4$	$f_2$	2440	1.50	
$\nu_1 + 2\nu_4$	$a_1 + e + f_2$	2168	1.37	
$2\nu_2 + \nu_3$	$f_1 + 2f_2$	2153	1.08	
$\nu_3 - \nu_1^h$	$f_2$	373	1.32	
$2\nu_3 - \nu_2^i$	$a_1 + e + f_2$	2131	0.61	
$3\nu_4 - \nu_2^i$	$a_1 + f_1 + 2f_2$	1459	3.07	

a. The matrix elements for the four fundamental transitions are the values calculated by Elliott and Ward from the infrared absorption data of Refs.(50-53). The remaining matrix elements were obtained from the overtone and combination band intensities read from the spectrum given in Ref.(50) and calibrated against the  $\nu_4$  band. The accuracy of the latter values is  $\pm 10-20\%$  at best. The transition dipole  $|\mu_{gm}^x|$  is nonzero for the  $f_2$  symmetry species only.

b. The polarizability matrix elements for the four fundamentals are essentially the values calculated by Elliott and Ward from the Raman scattering data of Refs.(54-57). The overtone intensities were measured in the course of the Raman spectroscopic assay of our sample. The intensities were calibrated against the intensity of the nearest fundamental of the same symmetry. The transition polarizability  $\alpha_{gm}^{xy}$  is nonzero for the  $f_2$  symmetry species only.

c. For this vibration of  $a_1$  symmetry the only nonzero transition polarizability is

$$1/3 |\alpha^{xx} + \alpha^{yy} + \alpha^{zz}| = 7.1 \times 10^{-42} \text{ C}^2 \text{m}^2 \text{J}^{-1} .$$

d. For this vibration of  $e$  symmetry the only nonzero transition polarizability is

$$|\alpha^{xx} - \alpha^{yy}| = 6.4 \times 10^{-42} \text{ C}^2 \text{m}^2 \text{J}^{-1} .$$

e. Since the  $2\nu_2$  band is strongly polarized and the  $a_1$  symmetry species is in Fermi resonance with  $\nu_1$ , one may assume that the intensity is dominated by the  $a_1$  species, giving

$$1/3 |\alpha^{xx} + \alpha^{yy} + \alpha^{zz}| = 1.44 \times 10^{-42} \text{ C}^2 \text{ m}^2 \text{ J}^{-1} .$$

f. This is an upper bound arrived at by assuming that the Raman intensity is due to only the  $f_2$  species.

g. Since the  $2\nu_4$  band is depolarized and the  $f_2$  species is in Fermi resonance with  $\nu_3$ , we assumed that the intensity is dominated by the  $f_2$  species.

h. Lower level is  $\nu_1 = 1$ .

i. Lower level is  $\nu_2 = 1$ .

## CHAPTER 6

## CONCLUSION

The experimental measurements of  $\gamma$  made by ESHG and a method for combining these measurements with those from other nonlinear optics experiments have been presented here. All the experimental data are consistent with the decomposition of  $\gamma$  into electronic and vibrational parts, where  $\gamma^e$  is strongly frequency dependent but  $\gamma^v$  is essentially constant for each nonlinear optical process. Combining measurements and theoretical calculations, one finds that for  $\text{CF}_4$ ,  $\gamma^v / \gamma^e = 1\%$ ,  $10\%$  and  $30\%$  corresponding to THG, ESHG and the dc Kerr effect respectively. This fact indicates that vibrational contributions to  $\gamma_{\text{CF}_4}$  are negligible for THG, but significant for both the dc Kerr effect and ESHG. Accurate data on the frequency dependence of  $\gamma_{\text{THG}}$  and  $\gamma_{\text{Kerr}}$  would allow a better test of the calculations and analysis in this thesis.

The estimate of the value of the hyper-Raman  $\beta$  of  $\text{CF}_4$  which is obtained as a by-product of this work allows one to predict that the hyper-Raman spectrum of  $\text{CF}_4$  will be 40x weaker than that of  $\text{CH}_4$ . A measurement of the hyper-Raman

spectrum of  $\text{CF}_4$  would provide another test of the above analysis. Ultimately, a measurement of  $\gamma_{\text{ESHG}}^{\text{V}}$  may provide a means for the accurate absolute calibration of the hyper-Raman  $\beta$ .

REFERENCES



- (1) Y.R. Shen, Principles of Nonlinear Optics (Wiley, New York, 1984)
- (2) M.D. Levenson, Introduction to Nonlinear Laser Spectroscopy (Academic, New York, 1982)
- (3) D.C. Hanna, M.A. Yuratich and D. Cotter, Nonlinear Optics of Free Atoms and Molecules (Springer, Berlin, 1979)
- (4) M.P. Bogaard and B.J. Orr, in International Review of Science, Physical Chemistry, Molecular Structure and Properties, edited by A.D. Buckingham (Butterworths, London, 1975), Ser. 2, Vol. 2, p.149
- (5) B.J. Orr and J.F. Ward, Mol. Phys. 20, 513 (1971)
- (6) N. Bloembergen, H. Lotem and R.T. Lynch, Ind. J. Pure Appl. Phys. 16, 151 (1978)
- (7) Y. Prior, IEEE J. Quant. Electron. 20, 3 (1984)
- (8) D.S. Elliott and J.F. Ward, Mol. Phys. 51, 45 (1984)
- (9) V. Mizrahi and D.P. Shelton, Phys. Rev. A 31, 3145 (1985)
- (10) D.P. Shelton, J. Chem. Phys. 84, 404 (1986)
- (11) L. Adamowicz and R.J. Bartlett, J. Chem. Phys. 84, 4988 (1986)
- (12) H. Sekino and R.J. Bartlett, J. Chem. Phys. 85, 976 (1986)
- (13) J.N. Silverman, D.M. Bishop and J. Pipin, Phys. Rev. Lett. 56, 1358 (1986)
- (14) G. Maroulis and D.M. Bishop, Mol. Phys. 58, 273 (1986)
- (15) M. Jaszunski and B.O. Roos, Mol. Phys. 52, 1209 (1984)
- (16) D.P. Shelton and A.D. Buckingham, Phys. Rev. A 26, 2787 (1982)
- (17) V. Mizrahi and D.P. Shelton, Phys. Rev. A 32, 3454 (1985)
- (18) V. Mizrahi and D.P. Shelton, Phys. Rev. Lett. 55, 696 (1985)
- (19) D.P. Shelton, Rev. Sci. Instrum. 56(7), 1474 (1985)
- (20) D.P. Shelton and V. Mizrahi, Chem. Phys. Lett. 120, 318 (1985)
- (21) D.P. Shelton, J. Chem. Phys. 85, 4234 (1986)
- (22) D.A. Long and L. Stanton, Proc. Roy. Soc. Lond. A. 318, 441 (1970)
- (23) S.J. Cyvin, J.E. Rauch and J.C. Decius, J. Chem. Phys. 43, 4083 (1965)

- (24) R. Bersohn, Y.-H. Pao and H.L. Frisch, J. Chem. Phys. 45, 3184 (1966)
- (25) K. Altmann and G. Strey, J. Raman Spectrosc. 12, 1 (1982)
- (26) S. Brodersen, in Topics in Current Physics, Raman Spectroscopy of Gases and Liquids, edited by A. Weber (Springer, Berlin, 1979), vol. 11, p.7.
- (27) J.F. Ward and I.J. Bigio, Phys. Rev. A 11, 60 (1975)
- (28) J.F. Ward and C.K. Miller, Phys. Rev. A 19, 826 (1979)
- (29) J.H. Dymond and E.B. Smith, The Virial Coefficients of Pure Gases and Mixtures, (Clarendon, Oxford, 1980)
- (30) D.P. Shelton and V. Mizrahi, Phys. Rev. A 33, 72 (1986)
- (31) Landolt-Bornstein, Zahlenwerte und Functionen, Band (II), Teil 8 (Spring) Berlin, 1962
- (32) T.K. Bose, J.S. Sochanski and R.H. Cole, J. Chem. Phys. 57, 3592 (1972)
- (33) K.L. Ramaswamy, Proc. Ind. Acad. Sci. Sect. A 2, 630 (1935)
- (34) P. Sitz and R. Yaris, J. Chem. Phys. 49, 3546 (1968)
- (35) D.P. Shelton, Phys. Rev. A 34, 304 (1986)
- (36) G.J. Rosasco and W.S. Hurst, J. Opt. Soc. Am. B 3, 1251 (1986)
- (37) A.D. Buckingham and B.J. Orr, Trans. Faraday Soc. 65, 673 (1969)
- (38) D.A. Dunmur, D.C. Hunt and N.E. Jessup, Mol. Phys. 37, 713 (1979)
- (39) R.S. Finn and J.F. Ward, J. Chem. Phys. 60, 454 (1974)
- (40) J.F. Ward and I.J. Bigio, Phys. Rev. A 11, 60 (1975)
- (41) J.F. Ward and D.S. Elliott, J. Chem. Phys. 80, 1003 (1984)
- (42) R.W. Terhune, P.D. Maker and C.M. Savage, Phys. Rev. Lett. 14, 681 (1965)
- (43) J.F. Verdieck and S.H. Peterson, Chem. Phys. Lett. 7, 219 (1970)
- (44) T.J. Dines, M.J. French, R.J.B. Hall and D.A. Long, J. Raman Spectrosc. 14, 225 (1983)
- (45) A.D. Buckingham and M.J. Stephen, Tran. Faraday Soc. 53, 884 (1957)
- (46) G. Herzberg, Infrared and Raman Spectra of Polyatomic

Molecules, (Van Nostrand, New York, 1945)

- (47) H.W. Schrotter and H.W. Klockner, in Topics in current Physics Raman Spectroscopy of Gases and Liquids, edited by A. Weber (Springer Berlin, 1979), Vol. 11, p.123
- (48) E.B. Wilson, J.C. Decius and P.C. Cross, Molecular Vibrations (Dover, New York, 1955)
- (49) D.A. Long, Raman Spectroscopy (McGraw-Hill, New York, 1977)
- (50) P.J.H. Waltz and A.H. Nielson, J. Chem. Phys. 20, 307 (1952)
- (51) P.N. Schatz and D.F. Hornong, J. Chem. Phys. 21, 1516 (1953)
- (52) I.W. Levin and T.P. Lewis, J. Chem. Phys. 52, 1608 (1970)
- (53) S. Saeki, M. Mizuno and S. Kondo, Spectrochim. Acta. 32A, 403 (1976)
- (54) B. Monostori and A. Weber, J. Chem. Phys. 33, 1867 (1960)
- (55) D.A. Long and E.L. Thomas, Trans. Faraday Soc. 59, 1026 (1963)
- (56) W. Holzer, J. Mol. Spectros. 25, 123 (1968)
- (57) R.S. Armstrong and R.J.H. Clark, J. Chem. Soc. Faraday Trans. II. 72, 11 (1976)

APPENDIX

PROGRAMS FOR THE CALCULATIONS

IN THE THESIS

```

0001          PROGRAM DENSITYCF4.FOR
0002
0003      C This program is used to calculate the density
0004      C of CF4.
0005      C B and C are the second and third virial
0006      C coefficient, respectively, in cm**3/mole and
0007      C cm**6/mole**2.
0008      C The input data are the pressure "P" in torr
0009      C and temperature "T" in "K".
0010      C The final output is the density of CF4 in
0011      C mole/m**3.
0012      C To exit the program type L=6.
0013      C To use this program for another gas, change
0014      C the virial coefficients B and C.
0015      B=-88.5
0016      C=6100
0017      1 WRITE (6,2)
0018      2 FORMAT (2X,23HPLEASE PUT IN DATA *P*.)
0019      3 READ (5,20) P
0020      4 WRITE (6,4)
0021      5 FORMAT (2X,23HPLEASE PUT IN DATA *T*.)
0022      6 READ (5,30) T
0023      7 WRITE (6,7)
0024      8 FORMAT (2X,40HPLEASE PUT IN THE DATA
0025      9 GROUP NUMBER *L*.)
0026      9 READ (5,40) L
0027      20 FORMAT (F10.4)
0028      30 FORMAT (F10.4)
0029      40 FORMAT (I1)
0030      50 D=P/(62363.68*T)
0031      DI=D/(1+B*D+C*D*D)
0032      DO 10 I=1,10
0033      DF=D/(1+B*DI+C*DI*DI)
0034      IF(ABS(DF-DI)-1E-8) 100,100,80
0035      80 DI=DF
0036      100 GOTO 10
0037      150 CONTINUE
0038      160 DF=DF*1E6
0039      180 WRITE (6,150)L,DF
0040      190 FORMAT (2X,3HCF4,2X,3HNO(,I1,1H),2X,
0041      200 BHDENSITY=,F10.4,2X,8HMOL/M**3)
0042      210 IF(L-5) 1,180,180
0043      220 STOP
0044      230 END

```

```

0001      PROGRAM AVD.FOR
0002
0003      C This program is used for fitting the data in an ESHG
0004      C experiment.
0005      C The experimental data are contained in the arrays
0006      C X(J) and Y(J) which are collected in the file
0007      C FDR003.DAT and read by AVD.FOR.
0008      C X(J) is the pressure (P) and Y(J) is the signal
0009      C count (S2w) at the corresponding pressure.
0010      C "N" is the degree of the fitting polynomial, chosen
0011      C by the user. "JI" is the number of data used. "P"
0012      C is the initial estimate of the peak pressure. The
0013      C values of "N", "JI" and "P" are to be entered following
0014      C a prompt by the program.
0015      C The program will give the coefficients of the normal
0016      C equations, the coefficients of the fitting polynomial,
0017      C the differences between the polynomial fit and
0018      C experimental data, X2 and the peak values of S2w and
0019      C P (divided by 1000). To exit the program, enter
0020      C N=16.
0021
0022      IMPLICIT REAL*8 (A-H,O-Z)
0023      DIMENSION X(15),Y(15),S(30),Q(30),T(20),
0024      DIMENSION A(20,20),B(20,20),R(15)
0025      DIMENSION E(15),P(15),D(15),AP(15),AY(15),
0026      DIMENSION SGA(15),RD(15),AAY(15),AAP(15),
0027      DIMENSION AD(15)
0028
0029      C READ THE DATA WHICH IS THE ORIGINAL DATA DIVIDE
0030      C BY 1000.
0031      C WRITE THE DATA.
0032      C J IS THE NUMBER OF THE DATA.
0033
0034      1 READ (003,10) (X(J),Y(J),J=1,10)
0035      10 FORMAT (1X,2F7.4)
0036      2 WRITE (6,5) (X(J),Y(J),J=1,10)
0037      5 FORMAT (2X,'P=',F6.4,5X,'S2W=',F7.3)
0038      21 WRITE (6,23)
0039      23 FORMAT (33H**PLEASE CHOOSE POWER NUMBER *N*.)
0040      25 READ (5,35) N
0041      IF (N-15) 26,26,300
0042      26 WRITE (6,27)
0043      27 FORMAT (33H**PLEASE CHOOSE DATA NUMBER *JI*.)
0044      READ (5,36) JI
0045      35 FORMAT (I2)
0046      36 FORMAT (I3)
0047
0048      C CALCULATE THE COEFFICIENTS OF THE NORMAL EQUATIONS.
0049
0050      37 WRITE (6,38)
0051      38 FORMAT (2X,3HTHE,1X,4HDATA,1X,2HOF,1X,
0052      13HM*S*EQUATIONS)
0053      45 NI=2*(N+1)
0054      DO 22 K=2,NI
0055      S(K)=0
0056      DO 11 J=1,JI
0057      S(K)=S(K)+X(J)**(K-2)
0058      CONTINUE
0059      Q(K)=S(K)
0060      WRITE (6,30) K,Q(K)
0061      CONTINUE
0062      22 FORMAT (10X,2HQ(,I2,2H)=,1X,D25.18)
0063      NN=N+1
0064      M=NN+1
0065      DO 44 K=1,NN

```

```

0058          T(K)=0
0059          DO 33 J=1,JI
0060          T(K)=T(K)+Y(J)*X(J)**(K-1)
0061          33  CONTINUE
0062          A(K,N+2)=T(K)
0063          B(K,N+2)=A(K,N+2)
0064          WRITE (6,40) K,N+2,B(K,N+2)
0065          44  CONTINUE
0066          40  FORMAT (10X,2HA(,I2,I2,2H)=,1X,D25.18)
0067          DO 55 I=1,NN
0068          DO 55 J=1,NN
0069          B(I,J)=S(I+J)
0070          WRITE (6,50) I,J,B(I,J)
0071          55  CONTINUE
0072          50  FORMAT (10X, 2HA(,I2,I2,2H)=,1X,D25.18)
0073
0074          C  A(I,J) IS THE COEFFICIENTS OF NORMAL EQUATIONS.
0075
0076          56  WRITE (6,57)
0077          57  FORMAT (2X,3HTHE,1X,12HCOEFFICIENTS,1X,
0078          60  WRITE (6,70) ((B(I,J),J=1,M),I=1,NN)
0079          70  FORMAT (2X,D24.18,3X,D24.18,3X,D24.18)
0080
0081          C  NOW SOLVE THE NORMAL EQUATIONS.
0082
0083          DO 66 K=1,NN
0084          BMAX=0
0085          DO 77 I=K,NN
0086          IF (BMAX-DABS(B(I,K))) 80,77,77
0087          80  BMAX=DABS(B(I,K))
0088          L=I
0089          77  CONTINUE
0090          EPS=1D-15
0091          IF (BMAX.LT.EPS) STOP4444
0092          IF (L.EQ.K) GOTO 90
0093          DO 88 J=K,M
0094          TT=B(L,J)
0095          B(L,J)=B(K,J)
0096          88  B(K,J)=TT
0097          90  TT=1.0/B(K,K)
0098          K1=K+1
0099          DO 99 J=K1,M
0100          B(K,J)=B(K,J)*TT
0101          DO 99 I=K1,NN
0102          99  B(I,J)=B(I,J)-B(I,K)*B(K,J)
0103          66  CONTINUE
0104          DO 111 IK=2,NN
0105          I=M-IK
0106          I1=I+1
0107          DO 111 J=I1,NN
0108          111 B(I,M)=B(I,M)-B(I,J)*B(J,M)
0109          112 DO 115 K=1,NN
0110          R(K)=B(K,M)
0111          WRITE (6,100) K,R(K)
0112          115 CONTINUE
0113          100 FORMAT (2X,8HSOLUTION,5X,
0114          2HS(,I2,2H)=,D24.18)

```

```

0115      C SOLUTION TO THE LEAST SQUARES PROBLEM HAS
0116      C BEEN OBTAINED.
0117      C R(K) IS THE COEFFICIENTS OF THE FIT FUNCTION.
0118      C NOW COMPARE THE SOLUTION WITH THE ORIGINAL DATA.
0119      WRITE (6,105)
0120      105      FORMAT (14X,8H*ERRORS*,23X,5H*SUM*)
0121      DO 222 I=1,JI
0122      XI=X(I)
0123      P(I)=0
0124      DO 333 K=1,NN
0125      QI=R(K)*XI**(K-1)
0126      P(I)=P(I)+QI
0127      333      CONTINUE
0128      AP(I)=DABS(P(I))
0129      AY(I)=DABS(Y(I))
0130      D(I)=DABS(AP(I)-AY(I))
0131      E(I)=D(I)/AP(I)
0132      WRITE (6,125) I,E(I),I,AP(I)
0133      125      FORMAT (10X,2HE(,I3,2H)=,D18.9,7X
0134      222      3HAP(,I3,2H)=,D18.9)
0135      CONTINUE
0136      C NOW ESTIMATE THE FIT FUNCTION.
0137      C AAP(I) IS THE FUNCTION VALUE.
0138      C AAY(I) IS THE DATA OF S2W.
0139      C XK IS CIGMA((Y-YI)**2/ABS(YI)).
0140      223      XK=0
0141      DO 331 I=1,JI
0142      AAP(I)=AP(I)*1000
0143      AD(I)=(D(I)*1000)
0144      RD(I)=AD(I)**2
0145      AAY(I)=AY(I)*1000
0146      XK=XK+RD(I)/AAY(I)
0147      331      CONTINUE
0148      133      WRITE (6,134) (RD(I),AAY(I),
0149      134      AAP(I),AD(I),I=1,JI)
0150      134      FORMAT (5X,'(Y-YI)**2=',D12.6,2X,
0151      + 'YI=',D12.6,2X,'Y=',D12.6,2X,
0152      332      'ABS(Y-YI)='F7.2)
0153      ND=JI-N-1
0154      CHI=XK/ND
0155      335      WRITE (6,335) XK,ND,CHI
0156      335      FORMAT (5X,'*SIGMA*=',D12.6,4X,
0157      + '*ND*=',I3,
0158      444      4X,'*CHISQ*=',F7.3)
0159      WRITE (6,110)
0160      DO 444 I=1,NN
0161      IR=I-1
0162      444      WRITE (6,120) IR,R(I)
0163      110      CONTINUE
0164      110      FORMAT (2X,36H THE COEFFICIENTS OF
0165      FIT*POLYNOMIAL)
0166      120      FORMAT (10X,2HR(,I2,2H)=,2X,D18.9)
0167      C NOW FIND THE PEAK.
0168      C XN IS THE INITIAL ESTIMATE.
0169      121      WRITE (6,122)
0170      122      FORMAT (2X,8H**PLEASE,1X,6HCHOOSE,
0171      130      1X,4H*P*.)
0172      READ (5,140)XN
0173      103      IF (XN.EQ.0.) ASSIGN 300 TO I

```



```

0172          IF (XN.EQ.22222.) ASSIGN 21 TO I
0173          IF (XN.LT.11111.) ASSIGN 145 TO I
0174          GO TO I,(300,21,145)
0175          140  FORMAT (F10.2)
0176          145  L=0
0177          EPX=1D-7
0178          150  L=L+1
0179          IF (L-200) 155,155,210
0180          155  X1=XN
0181          SUM=0
0182          DO 555 I=1,NN
0183          SMR=R(I)*X1**(I-1)
0184          SUM=SUM+SMR
0185          555  CONTINUE
0186          160  DSUM=0
0187          DO 666 J=2,NN
0188          DSMR=(J-1)*R(J)*X1**(J-2)
0189          DSUM=DSUM+DSMR
0190          666  CONTINUE
0191          161  DDSUM=0
0192          DO 667 K=3,NN
0193          DDSMR=(K-1)*(K-2)*R(K)*X1**(K-3)
0194          DDSUM=DDSUM+DDSMR
0195          IF (DDSMR) 667,210,667
0196          667  CONTINUE
0197          165  XN=X1-DSUM/DDSUM
0198          170  WRITE (6,190)
0199          WRITE (6,200) L,SUM,DSUM,XN
0200          175  AXN=DABS(XN)
0201          AX1=DABS(X1)
0202          DX=AXN-AX1
0203          IF (DABS(DX)-EPX) 220,220,150
0204          190  FORMAT (7X,1HL,13X,3HS2W,20X,4HDSUM,
0205          200  20X,1HP)
0206          210  FORMAT (5X,I4,4X,D18.9,4X,D18.9,4X,D18.9)
0207          WRITE (6,215)
0208          215  GOTO 130
0209          215  FORMAT (5X,7H*FAIL*.,4X,8H**PLEASE,1X,
0210          +      7HANOTHER,1X,2HP./5X,10H** 0= STOP/
0211          +      5X,25H**22222= CHOOSE ANOTHER N/
0212          220  5X,15H**<11111= GO ON)
0213          300  GOTO 21
0214          STOP
          END

```

```

0001          PROGRAM GAMA
0002
0003      C This program is used to calculate the
0004      C vibrational hyperpolarizability for the
0005      C dc Kerr effect. In the program, A, B,
0006      C and C are the data arrays corresponding
0007      C to  $\alpha_{uu}$ ,  $u\alpha_u$  and  $u\alpha_x$  terms, respectively.
0008      C The data for a single term specified by
0009      C A, B or C consists of three matrix
0010      C elements, two intermediate state
0011      C degeneracies and two transition
0012      C frequencies, in that order. The program
0013      C GAMA.FOR reads these data from the files
0014      C FOR051.DAT, FOR052.DAT and FOR053.DAT.
0015      C The output of the program is a list of
0016      C the input data, the calculated
0017      C contribution to the hyperpolarizability
0018      C for each term, and the final result for
0019      C the vibrational second hyperpolarizability
0020      C denoted by "GAMA".

0021          DIMENSION A(25,7),B(21,7),C(25,7),AA(25),
0022          + BB(25),CC(25)
0023
0024          READ (51,10) ((A(I,J),J=1,7),I=1,25)
0025          READ (52,20) ((B(I,J),J=1,7),I=1,21)
0026          READ (53,30) ((C(I,J),J=1,7),I=1,25)
0027      10      FORMAT (7F9.5)
0028      20      FORMAT (7F9.5)
0029      30      FORMAT (7F9.5)
0030          WRITE (6,11)
0031          WRITE (6,12) (I,(A(I,J),J=1,7),I=1,25)
0032      11      FORMAT (2X,'NO.',2X,'ALFA(gn)',5X,'U(np)',
0033          + ,5X,'U(pg)',3X,'g(n)',2X,'g(p)',3X,
0034          'U(gn)',4X,'U(pg)')
0035      12      FORMAT (2X,I2,2X,F9.5,2X,F9.5,2X,F9.5,2X,
0036          + F3.0,3X,F3.0,4X,F5.0,3X,F5.0)
0037          WRITE (6,22)
0038          WRITE (6,24) (I,(B(I,J),J=1,7),I=1,21)
0039      22      FORMAT (2X,'NO.',4X,'U(gm)',5X,'ALFA(mp)',
0040          + ,4X,'U(pg)',3X,'g(m)',2X,'g(p)',3X,
0041          'U(gm)',4X,'U(pg)')
0042      24      FORMAT (2X,I2,2X,F9.5,2X,F9.5,2X,F9.5,2X,
0043          + F3.0,3X,F3.0,4X,F5.0,3X,F5.0)
0044          WRITE (6,33)
0045      33      WRITE (6,36) (I,(C(I,J),J=1,7),I=1,25)
0046          FORMAT (2X,'NO.',5X,'U(gm)',5X,'U(mn)',
0047          + 4X,'ALFA(ng)',2X,'g(m)',3X,'g(n)',2X,'
0048          U(mg)',3X,'U(ng)')
0049      36      FORMAT (2X,I2,2X,F9.5,2X,F9.5,2X,F9.5,2X,
0050          + F3.0,3X,F3.0,4X,F5.0,3X,F5.0)
0051
0052      C NOW CALCULATE THE TERMS IN THE BRACKET OF GAMA.
0053
0054          X=9.123*1000
0055
0056      C PART (A). NO.1 - 25 DIVIDE BY 3
0057      C BECAUSE OF THE VIBERATIONAL SYMMETRY.

0058          SUMA=0
0059      41      DO 42 I=1,25

```

```

0058      AA(I)=X*A(I,1)*A(I,2)*A(I,3)*A(I,4)
0059      + *A(I,5)/(A(I,6)*A(I,7)*3.0)
0060      SUMA=SUMA+AA(I)
0061      42      CONTINUE
0062
0063      C PART (B). NO.1 - 15 DIVIDE BY 3 AND
          NO. 16 - 21 DIVIDE BY 9 BECAUSE OF
          C THE VIBERATIONAL SYMMETRY.
0064
0065      50      SUMB=0
          DO 55 I=1,15
0066      BB(I)=X*B(I,1)*B(I,2)*B(I,3)*B(I,4)*
0067      + B(I,5)/(B(I,6)*B(I,7)*3.0)
0068      SUMB=SUMB+2.0*BB(I)
0069      55      CONTINUE
0070      DO 56 I=16,21
0071      BB(I)=X*B(I,1)*B(I,2)*B(I,3)*B(I,4)*
0072      + B(I,5)/(B(I,6)*B(I,7)*9.0)
0073      SUMB=SUMB+2.0*BB(I)
0074      56      CONTINUE
0075
0076      C PART (C). SIMILAR TO PART (A).
0077
0078      60      SUMC=0
          DO 68 I=1,25
0079      CC(I)=X*C(I,1)*C(I,2)*C(I,3)*C(I,4)*
0080      + C(I,5)/(C(I,6)*C(I,7)*3.0)
0081      SUMC=SUMC+CC(I)
0082      68      CONTINUE
0083      WRITE (6,70) (I,AA(I),I, BB(I),I,
0084      CC(I),I=1,25)
0085      WRITE (6,75) SUMA,SUMB,SUMC
0086      70      FORMAT(2X,'A(',I2,')=',F9.6,3X,'B(
          ,I2,')=',
0087      + F9.6,3X,'C(',I2,')=',F9.6)
0088      75      FORMAT(4X,'SUMA=',F9.6,1X,'10**(-62)
          C4M4J-3',
0089      + /4X,'SUMB=',F9.6,1X,'10**(-62)C4M4J-3'
0090      + /4X,'SUMC=',F9.6,1X,'10**(-62)C4M4J-3')
0091      SUM=SUMA+SUMB+SUMC
0092      WRITE (6,80) SUM
0093      80      FORMAT(4X,'GAMA=',F9.6,1X,'10**
          (-62)C4M4J-3')
0094      90      STOP
0095      END
0096
0097

```